CHAPTER 1

AN EVALUATION OF THEORETICAL CALCULATIONS

Inelastic lepton-nucleon collision processes continue to be a subject of interest and importance in high energy particle physics. The process under present study is the production of hadrons (pions,kaons,nucleons,hyperons) in collision between an incident relativistic charge lepton (electron,muon) and a nucleon free or bound in an atomic nucleus. To have a physical insight, this process is viewed by using the concept of 'virtual quanta'. According to this point of view, the electromagnetic field of the incident relativistic particle is equivalent to the field of a pulse of radiation, This pulse of radiation represents a spectrum of virtual quanta. The effects (disintegration of nucleus, hadron production from virtual photon nucleon process, scattering) of these quanta are calculated and related to lepton-nucleon collision process to calculate the cross section of the particle process. This method developed independently by C.F. Weisacker and E.J. Williams in 1934 is now referred to as Williams-Weisacker (WW) semiclassical method.

In the late fifties, quantum electrodynamic (QED) treatment of single virtual photon exchange Feynman Dyson (FD) method was developed independently by a number of authors (Thie et al 1952, Kessler and Nase 1956,1957, Curtis 1957, Dalitz & Yennie 1957). In the sixties further developments have been made, among others by Diayasu et al (1962), Drell and Walecka (1964), Hand (1963), Sakurai (1969)

The main aim in all these treatments was to derive the differential cross section for the lepton-nucleon inelastic particle process. It appears necessary to make a critical evaluation of the various theoretical calculations in order to bring out their similarities and differences and to place in proper context the recent progress and the problems that remain unsolved.

We will begin by giving some basic kinematic relations. A brief derivation will then be presented of the semiclassical WW formula. A discussion will be given of the essential results of the QED treatments that are more familiar and useful for analysis of experiments. Emphasis will be on developments in late sixties. Much of the material will be covered rather rapidly, by excluding the most of the details in each treatment.

1.1. Basic formulae, Notations, Units

A bibliography of theoretical papers on the subject under study is given at the end of the thesis. Different notations have been used in these theoretical papers. For convenience, we use the same notation, the system of units and summarise some kinematic relations and initial formulae in this section.

We will consider hadron production in a collision between an incident relativistic 'muon' of charge 'e' and rest mass 'm' and a nucleon 'n' (for both proton and neutron) of the rest mass 'M'. For the incident particle, laboratory momentum, energy and velocity before and after collision are

$\bar{p}, E, v$ and $\bar{p}', E', v'$ respectively. The velocity is often expressed as $\beta = v/c$, where c is the velocity of light. Another convenient notation is $\gamma = (1-\beta^2)^{-1/2}$

The target nucleon at rest in the laboratory has momentum zero and energy equal to rest mass energy 'M'. So the laboratory momentum magnitude and energy of the incident particle are

$$p = \gamma m \beta c$$
$$E = \gamma m c^2 \qquad (1.1)$$

The momentum-energy four vector (four momentum of the incident particle)

$$p_\mu = \left(\bar{p}, i\frac{E}{c}\right), \qquad p_\mu' = \left(\bar{p}', i\frac{E'}{c}\right) \qquad (1.2)$$

For the target nucleon

$$P_\mu = \left(\bar{P}, i\frac{M}{c}\right) \quad \text{with} \quad \bar{P} = 0 \qquad (1.3)$$

For the virtual photon process in lepton-nucleon collision, the momentum and energy of the virtual photon are $\bar{q}, \epsilon$, given by

$$\bar{q} = \bar{p} - \bar{p}'$$
$$\epsilon = E - E' \qquad (1.4)$$

The corresponding four-momentum is

$$q = \left(\bar{q}, i\frac{\epsilon}{c}\right) \qquad (1.5)$$

The energy of the incident particle is expressed as

$$E = \left(p^2c^2 + m^2c^4\right)^{1/2}, \qquad E' = \left(p'^2c^2 + m^2c^4\right)^{1/2} \qquad (1.6)$$

To simplify by supressing powers of 'c' in energy and momentum expressions, rest mass, momentum and energy will be measured in energy units, the velocity of light being the unit (c=1) for velocity. With this convention and condition $p, p' \gg m$, we can write

$$E \approx p \quad , \quad E' \approx p' \tag{1.7}$$

The square of 'q', the virtual photon four momentum, denoted by 't' is

$$t \equiv q^2 = -(p'_\mu - p_\mu)^2$$
$$= -(p' - p)^2 + (E' - E)^2$$

In terms of laboratory scattering angle θ of the incident particle due to collision and using the approximation (1.7),

$$t = -2EE' + 2pp'\cos\theta + 2m^2$$

$$t - 2m^2 = -2EE'(1 - \cos\theta) = -4EE'\sin^2\frac{\theta}{2} \tag{1.8}$$

Using the approximation $p \approx E - \frac{1}{2}\frac{m^2}{E}$

$$t = -4EE'\sin^2\frac{\theta}{2} - m^2\left[\cos\theta\left(\frac{E}{E'} + \frac{E'}{E}\right) - 2\right] \tag{1.9}$$

At scattering angle zero, the minimum value of t is

$$t_{min} = -\frac{m^2\epsilon^2}{E(E-\epsilon)}$$

In absolute values,

$$t = 4EE'\sin^2\frac{\theta}{2} + 2m^2 \tag{1.10}$$

Under relativistic condition m^2 can be neglected

or
$$t = 4EE'\sin^2\frac{\theta}{2} \tag{1.11}$$

and
$$t_{min} = \frac{m^2\epsilon^2}{E(E-\epsilon)}$$

For the virtual photon process in the CM system of virtual photon and the nucleon, the square of the sum of virtual photon energy E_{vp}^{CM} and nucleon E_n^{CM} is defined as

$$\mathcal{E}^2 = \left(E_{vp}^{CM} + E_n^{CM}\right)^2 = -\left(q + p_\mu\right)^2 \qquad (1.12)$$

from this it is evident that

$$\mathcal{E}^2 = M^2 + 2M\epsilon - t$$

or
$$\frac{\mathcal{E}^2 - M^2}{2M} = \epsilon - \frac{t}{2M} \qquad (1.13)$$

For a real photon of laboratory energy K incident on the nucleon at rest

$$\mathcal{E}^2 = M^2 + 2MK \qquad (1.14)$$

or
$$K = \frac{\mathcal{E}^2 - M^2}{2M}$$

This means that if a photon, real or virtual, on absorption by a nucleon produces a final state with the same value of $\mathcal{E}$, it must have the energy K given by

$$K = \epsilon - \frac{t}{2M} \qquad (1.15)$$

So, for the virtual photon process the variables are K & t. In the $t = 0$ limit, $K = \epsilon$. K is the equivalent energy of virtual photon. From (1.15) it is evident that for elastic scattering when $K = 0$, the maximum value of t is

$$t_{max} = 2M\epsilon \qquad (1.16)$$

In the virtual photon process the effects of radiative process is related to the particle process. The initial formulae correlating the two processes written in form of differential with respect to the variable ϵ is

$$d\sigma(E,\epsilon) = N(E,\epsilon)\, d\epsilon\, \sigma_{\gamma n}(\epsilon)$$

$$\sigma(E) = \int_{\epsilon_{min}}^{E-m} N(E,\epsilon)\, \sigma_{\gamma n}(\epsilon)\, d\epsilon \qquad (1.17)$$

Where $d\sigma(E,\epsilon)$ is differential cross section of the muon-nucleon pion production process. $N(E,\epsilon)$ is the number of virtual photons of energy ϵ per unit energy. $\sigma_{\gamma n}(\epsilon)$ is the total cross section for absorption of photon (virtual) by the nucleon. The expression for $\sigma(E)$ is based on the assumption that the effect of virtual photons with various values of ϵ add incoherently. This is true only when the perturbing effects of fields of the incident particles are small so that both the incident and the struck particles remain almost undeflected after collision. So, the method is applicable under the condition

$$E \gg m \quad , \quad \epsilon \ll E \qquad (1.18)$$

1.2 Classical Williams-Weizsäcker (WW) method

E.J. Williams and C.F. Weizsäcker independently calculated using classical electrodynamics, the virtual photon spectrum (vps). The expression in William's paper (1935) is

$$N(E,\epsilon)\, d\epsilon = \frac{2}{\pi} \alpha \frac{d\epsilon}{\epsilon} \ln \frac{a E}{\epsilon} \qquad (1.19)$$

where $\alpha = \frac{1}{137}$ is the fine structure constant, a is a constant of the order of unity.

For convenience of presenting the subsequent developments, we will give a WW derivation of the vps.

We suppose that the incident particle moves along the

axix 3 (fig 1.1) and closest distance of approach (impact parameter) to the target nucleon 'n' is 'b'. (At time t = 0, the charge e is at 0, its distance from 'n' is b). According to classical electrodynamics, the electric and magnetic fields on 'n' are given as functions of t by

$$E_1(t) = \frac{\gamma e b}{(b^2+\gamma^2 v^2 t^2)^{3/2}}$$

$$E_3(t) = -\frac{\gamma e v t}{(b^2+\gamma^2 v^2 t^2)^{3/2}} \qquad (1.20)$$

$$B_2(t) = \beta E_1(t) \qquad (1.21)$$

The other components are vanishing.

For $\beta \simeq 1$, $\quad B_2(t) = E_1(t)$ (1.22)

It also follows that $E_1(t)$ and $B_2(t)$ are appreciable on 'n' over time interval

$$\Delta t \sim \frac{b}{\gamma v} \qquad (1.23)$$

As γ increases, the peak values of fields increase, but Δt decreases. As $\beta \to 1$, the nucleon 'n' sees nearly equal transverse and perpendicular E_1 and B_2 which are equivalent to a plane polarised pulse of radiation along axis 3. The field $E_3(t)$ has no magnetic component. If the target responds only to electric force, the necessary magnetic component can be taken for $E_3(t)$ to form a pulse of radiation moving along the direction of axis 1. This pulse is of minor importance for large γ.

A pulse of radiation can be analysed into a frequency spectrum using the Fourier transform of fields. For E (t) the Fourier transform is

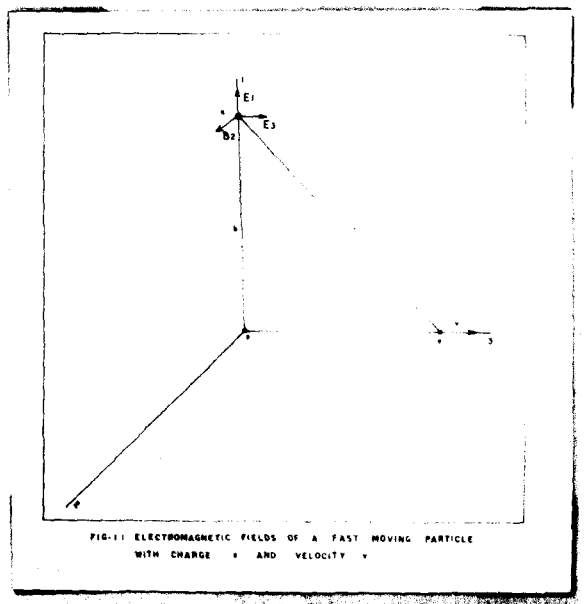

FIG-1.1 ELECTROMAGNETIC FIELDS OF A FAST MOVING PARTICLE WITH CHARGE e AND VELOCITY v

$$E(\omega) = \frac{1}{\sqrt{2\pi}} \int_{-\infty}^{+\infty} E(t)\, e^{i\omega t}\, dt \qquad (1.24)$$

The inverse is

$$E(t) = \frac{1}{\sqrt{2\pi}} \int_{-\infty}^{+\infty} E(\omega)\, e^{-i\omega t}\, d\omega \qquad (1.25)$$

Here ω is the frequency of radiation.

Using (1.20), (1.21)

$$E_1(\omega) = \frac{e}{bv} \left(\frac{2}{\pi}\right)^{1/2} \left[\frac{\omega b}{\gamma v} K_1\left(\frac{\omega b}{\gamma v}\right)\right] \qquad (1.26)$$

$$E_3(\omega) = -i \frac{e}{\gamma v b} \left(\frac{2}{\pi}\right)^{1/2} \left[\frac{\omega b}{\gamma v} K_0\left(\frac{\omega b}{\gamma v}\right)\right] \qquad (1.27)$$

$K_0\left(\frac{\omega b}{\gamma v}\right)$ and $K_1\left(\frac{\omega b}{\gamma v}\right)$ are modified Bessel functions.

The total energy flowing per unit area in the pulse of radiation formed by $E_1(t)$ and $B_2(t)$ is

$$W = \int_{-\infty}^{+\infty} \frac{c}{4\pi} \left[E_1(t) \cdot B_2(t)\right] dt$$

$$= \int_{-\infty}^{+\infty} \frac{c}{4\pi} \left[E_1(t)\right]^2 dt$$

using (1.25)

using (1.25) $W = \int_0^{\infty} \frac{c}{2\pi} |E_1(\omega)|^2\, d\omega \qquad (1.28)$

If $I_{Trans}(b,\omega)$ is the energy flow per unit area per unit frequency in the pulse of transverse (Trans) component E_1 then W can be expressed as

$$W = \int_0^{\infty} I_{Trans}(\omega, b)\, d\omega \qquad (1.29)$$

Comparing (1.28) and (1.29) we have

$$I_{Trans.}(\omega, b) = \frac{c}{2\pi} |E_1(\omega)|^2 \qquad (1.30)$$

Similarly, the pulse of the longitudinal (Long) component has frequency spectrum

$$I_{Long.}(\omega, b) = \frac{c}{2\pi} |E_3(\omega)|^2 \qquad (1.31)$$

The Fourier transform $E_1(\omega)$, $E_3(\omega)$ given by (1.26) and (1.27) are inserted in (1.30) and(1.31) to get the frequency spectra

$$\left.\begin{aligned} I_{Trans.}(\omega, b) &= \frac{1}{\pi^2}\frac{e^2}{c}\left(\frac{c}{v}\right)^2 \frac{1}{b^2}\left(\frac{\omega b}{\gamma v}\right)^2 K_1^2\left(\frac{\omega b}{\gamma v}\right) \\ I_{Long.}(\omega, b) &= \frac{1}{\pi^2}\frac{e^2}{c}\left(\frac{c}{v}\right)^2 \frac{1}{b^2}\frac{1}{\gamma^2}\left(\frac{\omega b}{\gamma v}\right)^2 K_0^2\left(\frac{\omega b}{\gamma v}\right) \end{aligned}\right\} \qquad (1.32)$$

The longitudinal spectrum $I_{Long.}$ is negligibly small (at very large γ when $v \approx c$). Since the width of pulse corresponding to $E_1(t)$ is $\Delta t \sim b/\gamma v$, the frequency spectrum $I_{Trans.}$ extends up to a maximum of the order

$$\omega_{max} \sim \frac{1}{\Delta t} = \frac{\gamma v}{b} \qquad (1.33)$$

The I_{Long} spectrum has a narrow range centering $\omega_{max} \sim \gamma v/b$

For frequencies less than $\gamma v/b$, that is,

$$\omega \ll \gamma v/b \quad \text{or} \quad \omega b/\gamma v \ll 1 \qquad (1.34)$$

We find approximately that

$$\left.\begin{aligned} E_1(\omega) &= \frac{e}{bv}\left(\frac{2}{\pi}\right)^{1/2}, \quad \omega b/\gamma v \ll 1 \\ E_1(\omega) &= 0, \quad \omega b/\gamma v \gg 1 \end{aligned}\right\} \qquad (1.35)$$

With this value of $E_1(\omega)$, the frequency spectrum $I_{Trans.}(\omega, b)$ is

$$I_{Trans.}(\omega, b) = \frac{1}{\pi^2} \frac{e^2}{c} \left(\frac{c}{v}\right)^2 \frac{1}{b^2} \tag{1.36}$$

To get $I_{Trans}(\omega)$, $I_{Trans.}(\omega, b)$ must be summed over the various possible impact parameter b. The upper value of b, determined by (1.34) is $b_{max} = \gamma v/\omega$. The lower value b_{min} is to be so chosen that for higher impact parameter, the incident particle fields are equivalent to a pulse of radiation, and for smaller impact parameter, this method is not useful. For the process of pion production on lepton-nucleon collision, b_{min} can be chosen as the radius of the target nucleon or $a \times \frac{\hbar}{mc}$ (a constant of the order of unity). Using $b_{min} = a\frac{\hbar}{mc}$

$$I_{Trans.}(\omega) = \frac{1}{\pi^2} \frac{e^2}{c} \left(\frac{c}{v}\right)^2 \int_{a\frac{\hbar}{mc}}^{\gamma v/\omega} \frac{1}{b^2} \cdot 2\pi b \, db$$

where

$$\epsilon = \hbar\omega \Big| \qquad = \frac{2}{\pi} \left(\frac{e^2}{c}\right) \left(\frac{c}{v}\right)^2 \ln \frac{\gamma v m c}{a\epsilon} \tag{1.37}$$

The transverse vpe $N(\epsilon)$ is obtained from by using the relation

$$I_{Trans.}(\omega)\, d\omega = \hbar\omega\, N(\hbar\omega)\, d(\hbar\omega)$$

$$= \epsilon\, N(\epsilon)\, d\epsilon \tag{1.38}$$

The result is

$$N(\epsilon)\, d\epsilon = \frac{2}{\pi} \propto \frac{d\epsilon}{\epsilon} \ln \frac{E}{a\epsilon} \tag{1.39}$$

when we put $v \simeq c$ & $c \simeq 1$ according to the adopted convention, the expression (1.38) is the same as (1.19) obtained by

Williams for the transverse virtual photon spectrum. If the contribution $I_{Long.}(\omega, b)$ is taken into account, the result without any approximation is

$$I(\omega) = 2\pi \int_{b_{min}}^{\infty} \left[I_{Trans.}(\omega, b) + I_{Long.}(\omega, b) \right] b \, db$$

$$= \frac{2}{\pi} \left(\frac{e^2}{c}\right) \left(\frac{c}{v}\right)^2 \left[\left(\frac{\omega b_{min}}{\gamma v}\right) k_0 \left(\frac{\omega b_{min}}{\gamma v}\right) k_1 \left(\frac{\omega b_{min}}{\gamma v}\right) \right.$$

$$\left. - \frac{1}{2} \left(\frac{\omega b_{min}}{\gamma v}\right)^2 \left\{ k_1^2 \left(\frac{\omega b_{min}}{\gamma v}\right) - k_0^2 \left(\frac{\omega b_{min}}{\gamma v}\right) \right\} \right] \qquad (1.40)$$

We can approximate this by

$$I(\omega) \simeq \frac{2}{\pi} \frac{e^2}{c} \left(\frac{c}{v}\right)^2 \left[\ln \frac{1.123 \, \gamma v}{\omega b_{min}} - \frac{1}{2} \frac{v^2}{c^2} \right], \quad \omega << \frac{\gamma v}{b_{min}}$$

(low frequency) (1.41)

$$I(\omega) \simeq \frac{e^2}{c} \left(\frac{c}{v}\right)^2 \left[1 - \frac{1}{2} \frac{v^2}{c^2} \right] e^{-\frac{2\omega b_{min}}{\gamma v}}, \quad \omega >> \frac{\gamma v}{b_{min}}$$

(high frequency) (1.42)

From low frequency approximation expression (1.41) we obtain, as before, with $v = c = 1$, the virtual photon spectrum

$$N(\epsilon) \, d\epsilon = \frac{2}{\pi} \alpha \frac{d\epsilon}{\epsilon} \left[\ln \frac{1.123 \, E}{\epsilon} + \ln \frac{\hbar}{m \, b_{min}} - \frac{1}{2} \right] \qquad (1.43)$$

This expression is similar to that obtained by Heitler (1954) and was used in earlier experimental work with different choices of b_{min} (Pagter and Sard 1960)

1.3 Treatments of Kessler and Kessler (1956), Kessler(1965)

The results of the theoretical treatment in the FD method by Kessler and Kessler (KK) have been used in several of the past experiments on multiple pion production in lepton-nucleon collision. The FD diagram of the process is shown in the fig. 1.2.

In the virtual photon process, one photon is exchanged between the scattered lepton and nucleon. The upper vertex describes the interaction between the lepton and virtual photon and the lower vertex describes the interaction between the virtual photon and the target nucleon. At the nucleon vertex one studies inelastic processes in which pions and other hadrons are produced.

One virtual photon exchange is assumed to dominate the process, since the exchange of a second photon is expected to be supressed by a factor of approximately $\frac{1}{137}$ (fine structure constant). Kessler and Kessler compared the virtual photon process with the real photon process (fig.1.2) to obtain under extreme relativistic condition ($E \gg m$) and small angle (lepton scattering angle and virtual photon emission angle) approximation, the following relation between $\sigma(E)$ and $\sigma_{\gamma n}(\epsilon)$

$$\sigma(E) = \frac{2\alpha}{\pi} \int \frac{d\epsilon}{\epsilon} \left[\left(1 - \frac{\epsilon}{E} + \frac{\epsilon^2}{2E^2}\right) \ln \frac{E-\epsilon}{m} - \frac{1}{2}\left(1 - \frac{\epsilon}{E}\right) \right] \sigma_{\gamma n}(\epsilon) \qquad (1.44)$$

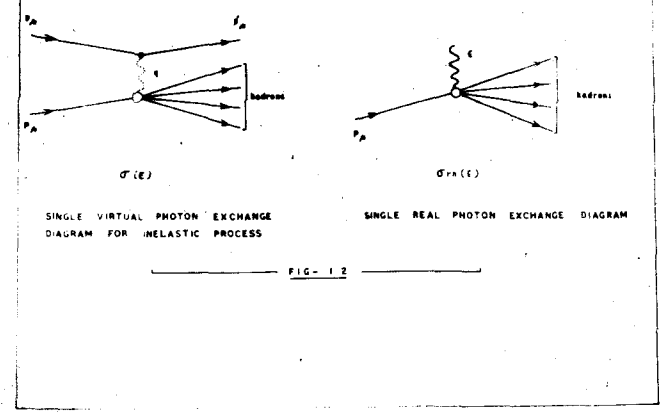

SINGLE VIRTUAL PHOTON EXCHANGE DIAGRAM FOR INELASTIC PROCESS

SINGLE REAL PHOTON EXCHANGE DIAGRAM

FIG- 1 2

From this the vps N(ϵ) is obtained as

$$N(\epsilon)\,d\epsilon = \frac{2\alpha}{\pi}\,\frac{d\epsilon}{\epsilon}\left[\left(1-\frac{\epsilon}{E}+\frac{\epsilon^2}{2E^2}\right)\ln\frac{E-\epsilon}{m}-\frac{1}{2}\left(1-\frac{\epsilon}{E}\right)\right] \tag{1.45}$$

The expressions for N(ϵ) obtained in the FD formalism by Curtis (1950) and Dalitz and Yennie (1957) are almost identical so far as the factor multiplying the logrithmic term is concerned. Differences occur only under logarithm and in other terms. These differences are not of much importance in actual numerical computation.

Kessler (1965) in a more exact formulation obtained the cross section differential in two variables ϵ and t. The result is

$$\frac{d^2\sigma}{d\epsilon\,dt} = N(E,\epsilon,t)\;\sigma_{\gamma n}(\epsilon,t) \tag{1.46}$$

with $N(E,\epsilon,t) = \frac{\alpha}{\pi}\,\frac{1}{(\epsilon^2+t)^{1/2}}\,\frac{1}{t}\left[1-\frac{\epsilon}{E}+\frac{\epsilon^2}{2E^2}+\frac{t}{4E^2}-\frac{m^2(\epsilon^2+t)}{tE^2}\right]$

The virtual photon-nucleon cross section $\sigma_{\gamma n}(\epsilon,t)$ has been assumed in several application to be of the form

$$\sigma_{\gamma n}(\epsilon,t) = \sigma_{\gamma n}(\epsilon)F(t) \tag{1.47}$$

$\sigma_{\gamma n}(\epsilon)$ is the total cross section for real photon absorption by the nucleon. The function $F(t) = (t_0/\,t_0+t)^2$ is the square of Hofstadter type nucleon electromagnetic form factor with $t_0 = 0.365$ (GeV)2 corresponding to a rms nucleon radius of 0.8 fm.

According to this procedure

$$F(t) = 1 \qquad \text{when } t \ll t_0$$

F(t) thus represents the influence of finite structure of the nucleon as function of t.

1.4 Treatment of Daiyasu, Kobayakawa, Kuroda, Nakano (DKKN) 1962

The authors have defined the cross section of the lepton-nucleon inelastic collision as a single photon exchange process by the expression

$$\frac{d^2\sigma}{d\epsilon\, dt} = N_{Trans}(\epsilon, t)\, L_{Trans}(\epsilon, t) + N_{Long}(\epsilon, t)\, L_{Long}(\epsilon, t)$$

Here $N_{Trans}(\epsilon, t)$, the transverse virtual photon flux is given by $N_T(\epsilon, t) = \frac{\alpha}{8\pi^2} \frac{1}{E^2 - m^2} \frac{1}{t^2} \left\{ E^2 t + (E-\epsilon)^2 t - 2m^2\epsilon^2 - \frac{t^2}{2} \right\}$

$N_{Long}(\epsilon, t)$, the longitudinal and scaler photon flux is

$$N_{Long}(\epsilon, t) = \frac{\alpha}{8\pi^2} \frac{1}{E^2 - m^2} \frac{1}{t^2} \left\{ (2m^2 - t)\, t \right\}$$

$L_{Trans}(\epsilon, t)$ and $L_{Long}(\epsilon, t)$ are corresponding functions, called structure functions, which are different from nucleon form factor. The authors assumed that

$$L_{Long}(\epsilon, t) = 0 \qquad (1.48)$$

$$L_{Trans}(\epsilon, t) = L_0 \left(\frac{t_0}{t_0 + t} \right)^2 = L_0 F(t) \qquad (1.49)$$

$$L_0 = \frac{4\pi}{\epsilon} \sigma_{\gamma n}(\epsilon)$$

The value of t_0, the cut off parameter in the nucleon form factor is chosen 0.365 $(GeV)^2$ corresponding to the rms nucleon radius of 0.8 fm.

For a point nucleon, $t_o \to \infty$

$$F(t) = 1$$

$$L_{Trans}(\epsilon, t) = \frac{4\pi}{\epsilon} \sigma_{\gamma n}(\epsilon)$$

$$and \quad \frac{d^2\sigma}{d\epsilon\, dt} = 4\pi N_{Trans}(\epsilon, t) \frac{\sigma_{\gamma n}(\epsilon)}{\epsilon} \qquad (1.50)$$

For a cloud like nucleon, t_o, finite

$$\frac{d^2\sigma}{d\epsilon\, dt} = 4\pi N_{Trans}(\epsilon, t) \frac{\sigma_{\gamma n}(\epsilon)}{\epsilon} \left(\frac{t_o}{t_o+t}\right)^2 \qquad (1.51)$$

Kobayakawa (1967), one of the authors of DKMN treatment, put the cross section in the following form by introducing the experimentally indicated (Higashi et al 1965) probabilities of point like and cloud like nucleon structures. His formula is

$$\frac{d^2\sigma}{d\epsilon\, dt} = 4\pi N_{Trans}(\epsilon, t) \left\{ a + (1-a)\left(\frac{t_o}{t_o+t}\right)^2 \right\} \frac{\sigma_{\gamma n}(\epsilon)}{\epsilon} \qquad (1.51)$$

where the factor 'a' gives the contribution from point like structure. Kobayakawa suggested a=0.1 on the basis of experimental data of Higashi et al(1965).

1.5 Treatments based on single virtual photon exchange through a vector meson, vector meson-dominance (vmd) model.

These treatments are based on the concept that the virtual photon couples to the nucleon through a vector meson (ρ, ω, φ) and the strength of the coupling is independent of t. The diagram of the virtual process is shown in the fig. 1.5

That a vector meson may be expected to play such a

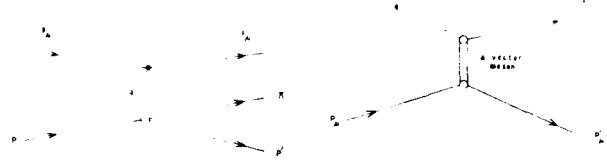

FIG-1.3 SINGLE VIRTUAL PHOTON PROCESS THROUGH A VECTOR MESON FOR SINGLE PION PRODUCTION

role has experimental support (Hoffman et al 1969, Dietrie et al 1969, Perl et al 1969). The experiments (Bishop 1962, Hand et al 1962) on the electric charge and magnetic moment distribution on nucleon by high energy electron scattering have given nucleon electric and magnetic form factors as function of 't'. The experimental data favour the assumption of one photon exchange process in the scattering process and permit evaluation of isovector and isoscalar form factors. For isovector electric and magnetic form factors, the following expressions have been obtained

$$G_E^V(t) = -0.4 + \frac{0.9\, t_0}{t_0 + t}$$

$$G_M^V(t) = -1.0 + \frac{3.4\, t_0}{t_0 + t} \qquad (1.53)$$

with $(t_0)^{1/2} = 750$ MeV

This is the same as the mass of the neutral ρ^0-meson. The result points to the conjecture that the structure of the nucleon has something to do with the existence of these ρ^0, ω, φ multi-pion resonances. An analysis regarding the possibility of such connection shows that the nucleon form factors which are determined by electromagnetic current operator must contain terms like that in (1.53) with 't_0' corresponding to the mass of the resonating state (matrix element of the electromagnetic current operator is large for resonances in multi-pion system such as ρ^0, ω, φ mesons). For isovector form factor this mass should be mass of ρ^0-meson and this is consistent with the observation. The isoscalar form factor has to be estimated using the mass of ω-meson.

We now present the results of various calculations using the concept of vector meson dominance.

(a) Method of Drell and Walecka (1964)

The general expression for the inelastic lepton-nucleon cross section was obtained by them in the following form

$$\frac{d^2\sigma}{d\epsilon dt} = \frac{4\pi\alpha^2}{t^2}\frac{E'}{E}\left[W_2(\epsilon,t) + 2W_1(\epsilon,t)\sin^2\theta/2\right] \qquad (1.55)$$

where the inelastic form factor (also called structure function) given by

$$W_1 = \frac{1}{4\pi^2\alpha}\left(\epsilon^2+t\right)^{1/2}\sigma_{Trans}(\epsilon,t) \qquad (1.56)$$

$$W_2 = \frac{1}{4\pi^2\alpha}\frac{t}{(\epsilon^2+t)^{1/2}}\left[\sigma_{Trans}(\epsilon,t) - \sigma_{Long}(\epsilon,t)\right] \qquad (1.57)$$

σ_{Trans} and σ_{Long} are the cross sections for absorption by the nucleon of transverse and longitudinal photons. According to Bjorken (1969) these form factors, at high values of and t should only be function of the ratio of these two variables. For W_2, he suggested

$$W_2 = \frac{1}{\epsilon}F\left(\frac{2M\epsilon}{t}\right)$$

where the function $F\left(\frac{2M\epsilon}{t}\right)$ is conjectured to manifest 'scale invariance' in sense that it depends only on the ratio $\frac{\epsilon}{t}$; using (1.11)

$$\frac{d^2\sigma}{d\epsilon dt} = \frac{4\pi\alpha^2}{t^2}\frac{1}{E^2}\left[\frac{1}{2}t\,W_1(\epsilon,t) + \left(E^2 - E\epsilon - \frac{t}{4}\right)W_2(\epsilon,t)\right] \qquad (1.58)$$

according to v m d model, the dependence of σ_{Trans} and σ_{Long} on t is assumed to be given by the square of the neutral vector meson propagator.

For ρ^0-meson of mass m_ρ, the virtual photon absorption cross sections were taken as

$$\sigma_{Long}(\epsilon, t) = 0 \tag{1.59}$$

$$\sigma_{Trans}(\epsilon, t) = \sigma_{\gamma n}(\epsilon) \left(\frac{m_\rho^2}{m_\rho^2 + t}\right)^2 \tag{1.60}$$

using these forms for σ_{Long} and σ_{Trans}, (1.58) is expressed as

$$\frac{d^2\sigma}{d\epsilon\, dt} = \frac{\alpha}{2\pi} \frac{1}{t} \frac{1}{E^2} \left[\left(t + \epsilon^2\right)^{\gamma_2} + \frac{2EE' - \frac{1}{2}t}{\left(t+\epsilon^2\right)^{\gamma_2}} \right] \sigma_{\gamma n}(\epsilon) \left(\frac{m_\rho^2}{m_\rho^2 + t}\right)^2$$

This can be reduced to

$$\frac{d^2\sigma}{d\epsilon\, dt} = \frac{\alpha}{\pi} \frac{1}{t} \frac{1}{\left(t+\epsilon^2\right)^{\gamma_2}} \left\{ 1 - \frac{\epsilon}{E} + \frac{1}{2} \frac{\epsilon^2}{E^2} \right\} \sigma_{\gamma n}(\epsilon) \left(\frac{m_\rho^2}{m_\rho^2 + t}\right)^2 \tag{1.61}$$

The total photon-nucleon absorption cross sections $\sigma_{\gamma n}(\epsilon)$ is given (von Bochmann and Margolis, 1969) by

$$\sigma_{\gamma n}(\epsilon) = \frac{\alpha}{4} \sum_{v = \rho, \omega, \varphi} \left(\frac{\gamma_v^2}{4\pi}\right)^{-1} \sigma_{vn} \tag{1.62}$$

where γ_ρ is the ρ- photon coupling constant and $\sigma_{\rho n}$ is the ρ - nucleon cross section. Using this formula, Caldwell et al (1969) derived ρ- nucleon coupling constant from the measured value of $\sigma_{\gamma n}$ (for photo-absorption by protons) and $\sigma_{\rho n}$. The result is $\frac{\gamma_\rho^2}{4\pi} = 0.38$, assuming that ω and ρ - mesons contribute 18 μb to the $\sigma_{\gamma n}$. Anderson et al (1969) obtained $\frac{\gamma_\rho^2}{4\pi} = 0.42$, assuming ω and φ contribution of 18 μb to $\sigma_{\gamma n}$ and using the ρ- meson dominance relation

$$\sigma_{\gamma n} = \left[4\pi\alpha \frac{4\pi}{\gamma_\rho^2} \frac{d\sigma}{dt} \left(\gamma n - \rho n\right)_{t=0} \right]^{\gamma_2} \tag{1.63}$$

(b) Calculation of Sakurai (1969)

Sakurai calculated ρ- proton cross section for transversely and longitudinally polarised ρ-mesons and obtained in terms of these cross sections, transverse and scalar photon cross sections σ_T , σ_S , according to the formulation by Hand (1963). Transverse and scalar photon cross sections are related to σ_T and σ_S as

$$\sigma_T = \frac{|\bar{q}|}{K}\,\sigma_{Trans}$$
$$\sigma_S = -\frac{|\bar{q}|}{K}\,\sigma_{Long} \qquad (1.64)$$

The expressions for σ_T, σ_S , as obtained by Sakurai, are

$$\sigma_T(\epsilon,t) = \left(\frac{e}{f_\rho}\right)^2\left(\frac{m_\rho^2}{m_\rho^2+t}\right)^2 \sigma_{\rho n}^{(\perp)}(K) \qquad (1.65)$$

where
$$\sigma_S(\epsilon,t) = \left(\frac{e}{f_\rho}\right)^2\left(\frac{m_\rho^2}{m_\rho^2+t}\right)^2 \frac{t}{m_\rho^2}\left(\frac{K}{\epsilon}\right)^2 \xi(K)\,\sigma_{\rho n}^{(\parallel)}(K) \qquad (1.66)$$

$$\xi(K) = \frac{\sigma_{\rho n}^{(\parallel)}}{\sigma_{\rho n}^{(\perp)}}$$

The ratio σ_S/σ_T is $R = \dfrac{\sigma_S(\epsilon,t)}{\sigma_T(\epsilon,t)} = \xi(K)\dfrac{t}{m_\rho^2}\left[1-\dfrac{t}{2M\epsilon}\right]^2$ (1.67)

Sakurai then calculated W_1 and W_2 by putting

$$\sigma_{\gamma n}(K) = \left(\frac{e}{f_\rho}\right)^2 \sigma_{\rho n}^{(\perp)}(K) \qquad (1.68)$$

In terms of σ_T and σ_S

$$W_1 = \frac{K}{4\pi^2\alpha}\,\sigma_T = \frac{K}{4\pi^2\alpha}\,\sigma_{\gamma n}(K)\left(\frac{m_\rho^2}{m_\rho^2+t}\right)^2 \qquad (1.69a)$$

$$W_2 = \frac{K}{4\pi^2\alpha}\,\frac{t}{(t+\epsilon^2)}\left(\sigma_T + \sigma_S\right)$$
$$= \frac{K}{4\pi^2\alpha}\,\frac{t}{t+\epsilon^2}\,\sigma_{\gamma n}(K)\left[\frac{m_\rho^2}{m_\rho^2+t}\right]^2 \times$$
$$\left[1 + \frac{t}{m_\rho^2}\left(\frac{K}{\epsilon}\right)^2 \xi(K)\right] \qquad (1.69b)$$

For $\xi(K) \approx 1$ (if high energy ρ- nucleon interaction is spin independent) and $K \approx \epsilon$

$$W_2 \simeq \frac{K}{4\pi^2\alpha} \frac{t}{t+\epsilon^2} \sigma_{\gamma n}(K) \frac{m_\rho^2}{m_\rho^2+t} \qquad (1.70)$$

Substituting for W_1 and W_2 in eqn. (1.55) and neglecting $2m^2$ we get

$$\frac{d^2\sigma}{d\epsilon dt} = \frac{\alpha}{2\pi} \frac{K}{t} \frac{1}{E^2} \left(\frac{m_\rho^2}{m_\rho^2+t} + \frac{2EE' - t/2}{t+\epsilon^2} \right) \sigma_{\gamma n}(K) \frac{m_\rho^2}{m_\rho^2+t} \qquad (1.71)$$

Detailed calculation leads to the expression

$$W_2 = \frac{K}{4\pi^2\alpha} \frac{m_\rho^2}{\epsilon^2} \frac{1}{1+t/\epsilon^2} \left[\frac{1}{1+\frac{m_\rho^2}{t}} \right]^2 \times \left[\frac{m_\rho^2}{t} + \xi(K) \left(\frac{K}{\epsilon} \right)^2 \right] \sigma_{\gamma n}(K)$$

$$\epsilon W_2 = \frac{K}{4\pi^2\alpha} \frac{m_\rho^2}{\epsilon} \frac{1}{1+\frac{t}{\epsilon^2}} \left[\frac{1}{1+\frac{m_\rho^2}{t}} \right]^2 \times \left[\frac{m_\rho^2}{t} + \xi(K) \left(\frac{K}{\epsilon} \right)^2 \right] \sigma_{\gamma n}(K)$$

(1.72)

This shows for fixed values of ϵ/t and $\xi = 1$, the variation of ϵW_2 as t increases. Its value is lower than the Bjorken limit (Bjorken 1969) even at $t = 4$ (GeV)^2 by about 15 %. If ξ is slightly higher, the approach to Bjorken limit is slower. We now find an expression for inelastic lepton-nucleon cross section using Hand's definition of this, for one virtual photon exchange process (fig. 1.2). According to Hand (1963)

$$\frac{d^2\sigma}{dK dt} = N_T(K,t)\, \sigma_T(K,t) + N_S(K,t)\, \sigma_S(K,t)$$

$$= N_T(\sigma_T + \epsilon\sigma_S) = N_T \sigma_T (1 + \epsilon R)$$

(1.73)

Where N_T, N_S, the transverse and scalar virtual photon fluxes, are given by

$$N_T(K,t) = \frac{\alpha}{2\pi t}\left(\frac{K}{p^2}\right)\left(1 - \frac{2m^2}{t} + \frac{2EE' - \frac{1}{2}t}{(E-E')^2 + t}\right) \tag{1.74}$$

$$N_S(K,t) = \frac{\alpha}{2\pi t}\left(\frac{K}{p^2}\right)\frac{2EE' - \frac{1}{2}t}{(E-E')^2 + t} \tag{1.75}$$

$$\epsilon = N_S/N_T = \left[\frac{1 - \frac{2m^2}{t} + \frac{2EE' - \frac{1}{2}t}{(E-E')^2 + t}}{\left(2EE' - \frac{1}{2}t\right)\left\{(E-E')^2 + t\right\}}\right]^{-1} \tag{1.76}$$

$$R = \sigma_S/\sigma_T = \xi(K)\frac{t}{m_\rho^2}\left[1 - t/2M\epsilon\right]^2 \tag{1.77}$$

using (1.76, 1.77) we get cross section in the form

$$\frac{d^2\sigma}{dK\,dt} = N_T(K,t)\,\sigma_{\gamma n}(K)\left(1 + \frac{t}{m_\rho^2}\right)^{-2}\left[1 + \epsilon\,\xi(K)\frac{t}{m_\rho^2}\left(\frac{K}{\epsilon}\right)^2\right]$$

$$= N_T(K,t)\,\sigma_{\gamma n}(K)\left(1 + \frac{t}{m_\rho^2}\right)^{-2}\left[1 + \frac{t}{m_\rho^2}\epsilon\,\xi(K)\left(\frac{K}{K + \frac{t}{2M}}\right)^2\right] \tag{1.78}$$

with $\xi \approx 1$, $\epsilon \approx 1$, from experiments of Hoffman et al(1969) Dieterle et al (1969) and Perl et al (1969) and $K \gg \frac{t}{2M}$ $\left(\frac{K}{t} \gg \frac{1}{2M}\right)$, the expression simplifies to

$$\frac{d^2\sigma}{dK\,dt} = N_T\,\sigma_{\gamma n}(K)\left(1 + \frac{t}{m_\rho^2}\right)^{-1} \tag{1.79}$$

The process of reducing eqn. (1.73) to eqn. (1.79) means the assumption

$$\frac{\sigma_S}{\sigma_T} = \frac{t}{m_\rho^2} \qquad (1.80)$$

Inclusion of σ_S in the calculation results in the cross section dependent on ρ- meson propagator instead of on the square of the ρ- meson propagator.

(c) Calculations of Crossland and Fowler (1964)

The single pion production process (fig. 1.3) was treated using the model of virtual photon interaction with the nucleon mainly via a vector meson. The ρ^0 or ω meson is characterised by a Regge trajectory and the differential cross section of the process in variables ϵ & t, is expressed in terms of $\sigma_{Trans}(\epsilon^2, t)$ and $\sigma_{Long}(\epsilon^2, t)$. They have not given separate expressions for $\sigma_{Trans}(\epsilon^2, t)$ and $\sigma_{Long}(\epsilon^2, t)$ and have given under high energy approximation a formula involving a form factor

$$|F(t)|^2 = \left(\frac{\Lambda^2}{\Lambda^2 + t}\right)^2 \times (a + bt + ct^2) \qquad (1.81)$$

$\Lambda^2 = 1\ (GeV)^2$

The coefficients a, b, c, are functions of 't'. Their results concern single pion production whereas the most of the experimental data concern production of multiple pions.

1.6 Numerical calculation of cross sections

The existing experimental data for muon-nucleon inelastic process concern total cross-sections and also differential cross-section only in few cases. In the present work, we have performed numerical calculation of theoretical cross-sections from the treatments:

(i) vmd model formulation, expression (1.79)

(ii) DKMM formulation, expression (1.52)

(iii) Kessler formulation, expression (1.46)

(iv) KK formulation, expression (1.44)

(v) WW formulation, expression (1.43)

The steps in the computational procedure are the evaluations for each of large number of muon energies in the range 1 GeV to 10 TeV, of

a. $\frac{d^2\sigma}{d\epsilon\, dt}(E, \epsilon, t)$

b. $\frac{d\sigma}{d\epsilon}(E,\epsilon) = \int \frac{d^2\sigma}{d\epsilon\, dt}\, dt$

c. $\frac{d\sigma}{dt}(E, t) = \int \frac{d^2\sigma}{d\epsilon\, dt}\, d\epsilon$

d. $\sigma(E, > \epsilon) = \int_{\epsilon}^{\epsilon_{max}} \frac{d\sigma}{d\epsilon}\, d\epsilon$

e. $\sigma(E, > t) = \int_{t}^{t_{max}} \frac{d\sigma}{dt}\, dt$.

The limits of t and ϵ are the following

$$t_{min} = \frac{\epsilon^2 m^2}{E(E-\epsilon)} \qquad t_{max} = 2M\epsilon$$

$$\epsilon_{min} = 0 \qquad \epsilon_{max} = E - M\left\{1 + \left(\frac{m^2}{M^2}\right)\right\}/2$$

where $M(1 + \frac{m^2}{M^2})/2 = 0.475$ GeV

In the computation, we have used photo-nuclear cross sections $\sigma_{\gamma n}(K)$ as a function of ϵ as given by recent experiments (fig. 1.4) upto photon energy of about 17 BeV. The experimental direct photo-nucleon absorption cross section data are also in agreement with those derived from the vmd model-fit to muon-proton inelastic scattering data of Perl et al (1969). The theoretical calculations of total photo-nucleon absorption cross section on the basis of vector dominance model (Davier et al 1968, von Boehmann and Margolis 1969) and Regge-Pole model (Bussolla & Colocci 1967) have given results consistent with experiments upto photon energy of 100eV. The new experiments (Beznukov et al 1972, Chin et al 1973) on the production of very high energy penetrating showers have not indicated any significant deviation from the trend of cross section shown in fig. 1.4.

In the numerical integration, interpolation was necessary. The error of interpolation was within 1-2%.

A selection of the various computed cross sections are presented in figures 1.5 - 1.32; we have also given tables (1.1 - 1.21) of cross sections for a selection of muon energies for numerical comparisions of various predicted cross sections. To show the differences in these cross sections the ratio of cross sections according to various formulations relative to the cross sections of vmd - Sakurai is plotted in figs. 1.33 - 1.37.

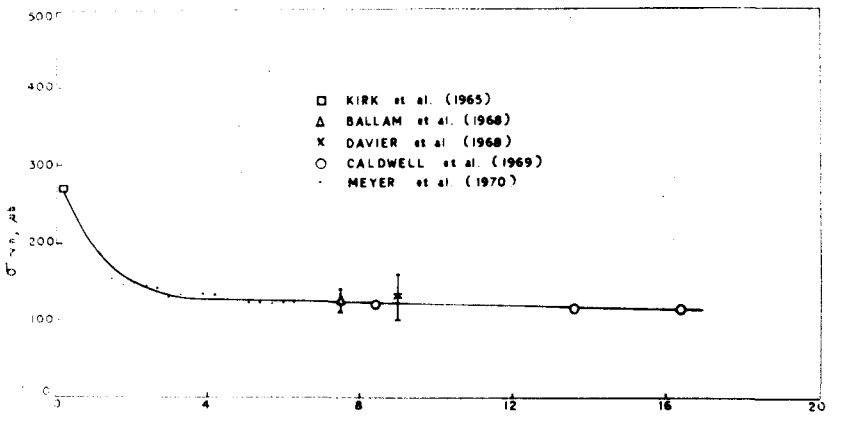
500
400
300
200
100
0
0
4
8
12
16
20
□ KIRK et al. (1965)
Δ BALLAM et al. (1968)
× DAVIER et al. (1968)
○ CALDWELL et al. (1969)
· MEYER et al. (1970)
REAL PHOTON ENERGY, GeV

FIG-1·4

In case of v n d (Sakurai) theory the energy transfer variable is K in the following figures 1.5 to 1.13.

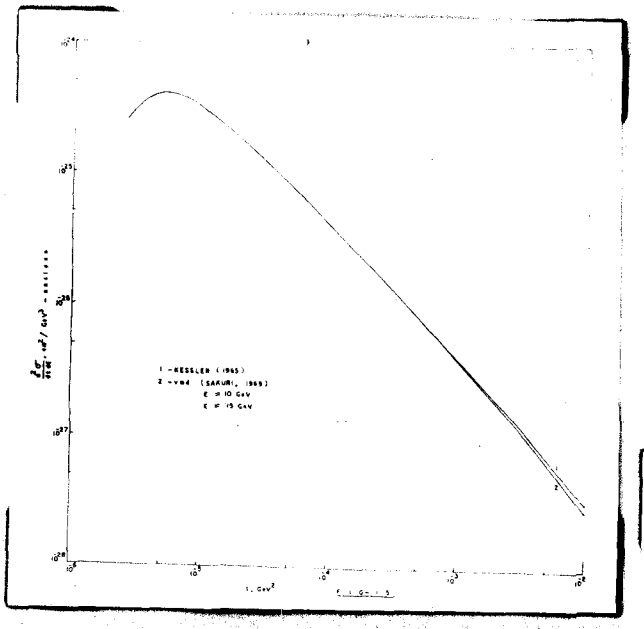

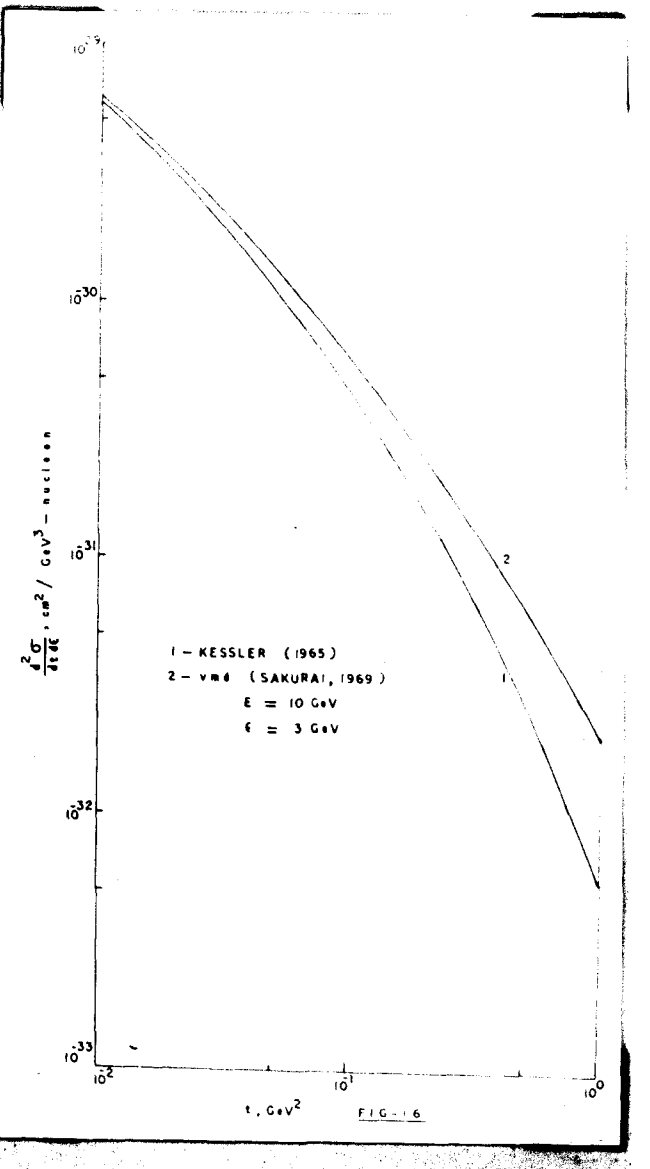

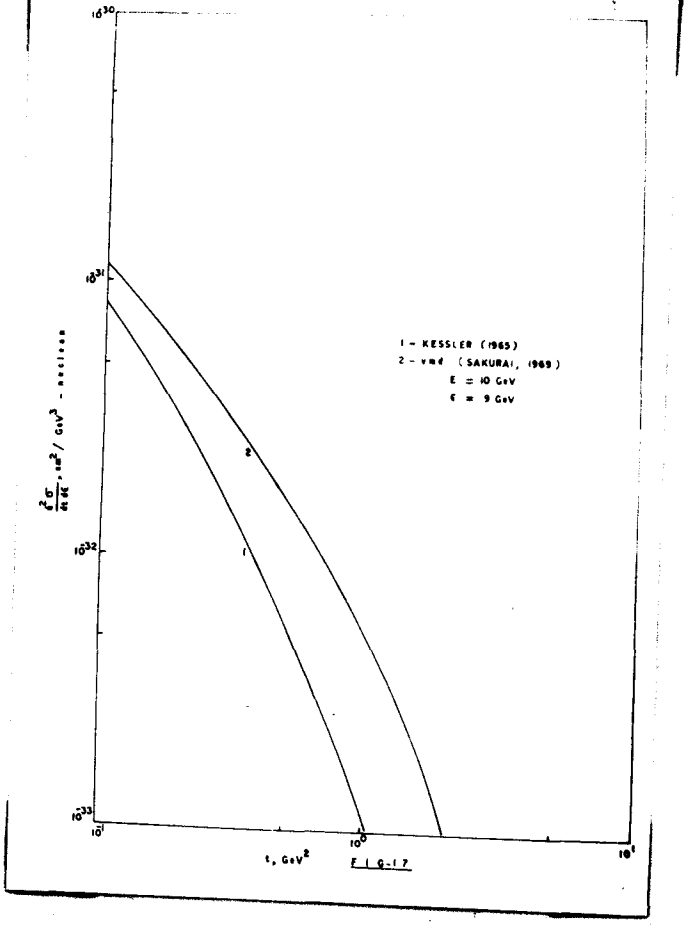
1 - KESSLER (1965)
2 - νμd (SAKURAI, 1969)
E = 10 GeV
ε = 9 GeV
t, GeV²

FIG-17

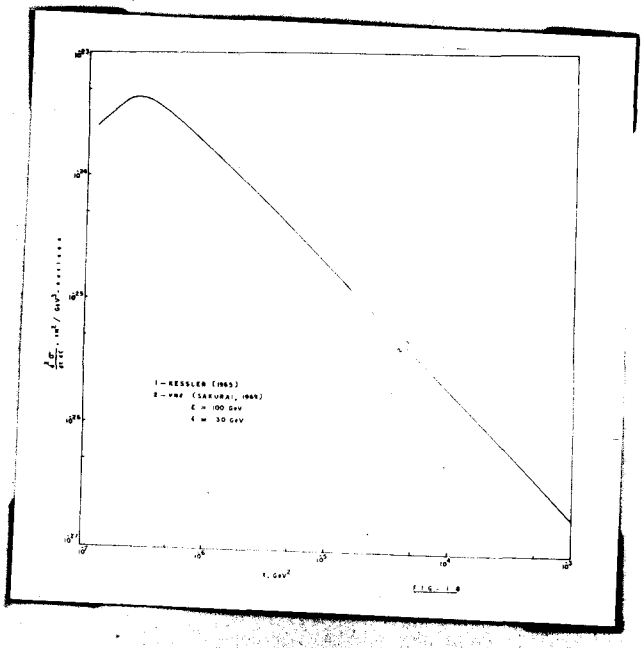
1 - KESSLER (1965)
2 - νμd (SAKURAI, 1969)
E = 100 GeV
ε = 30 GeV
t, GeV²

FIG-18

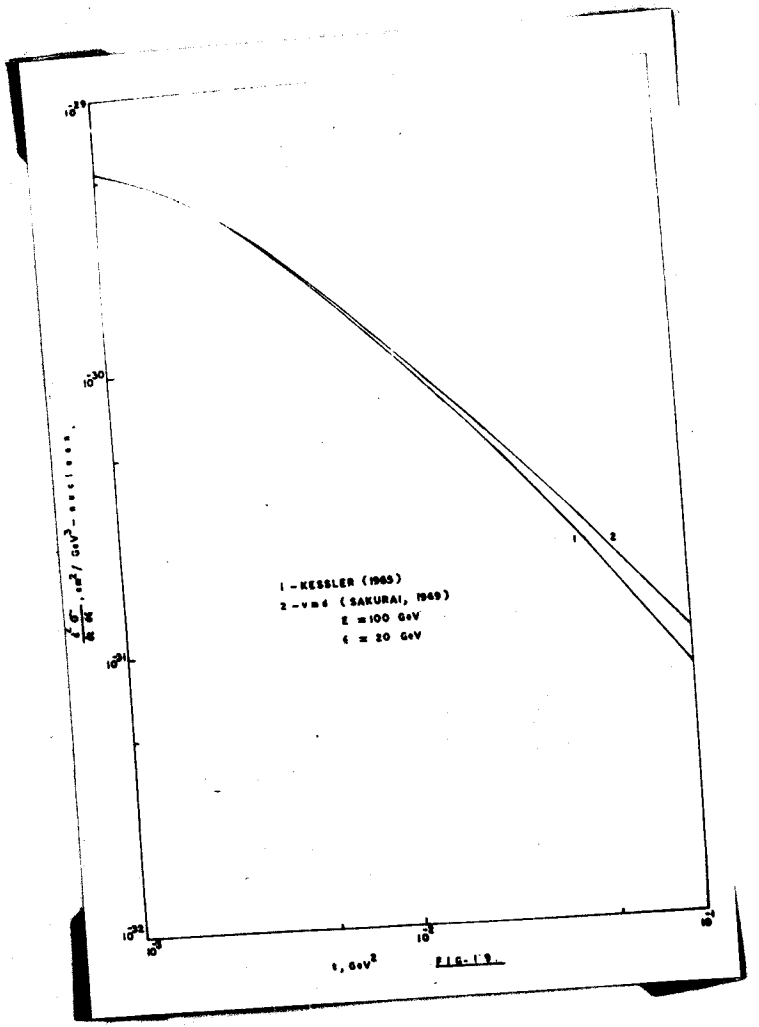

FIG-1.9

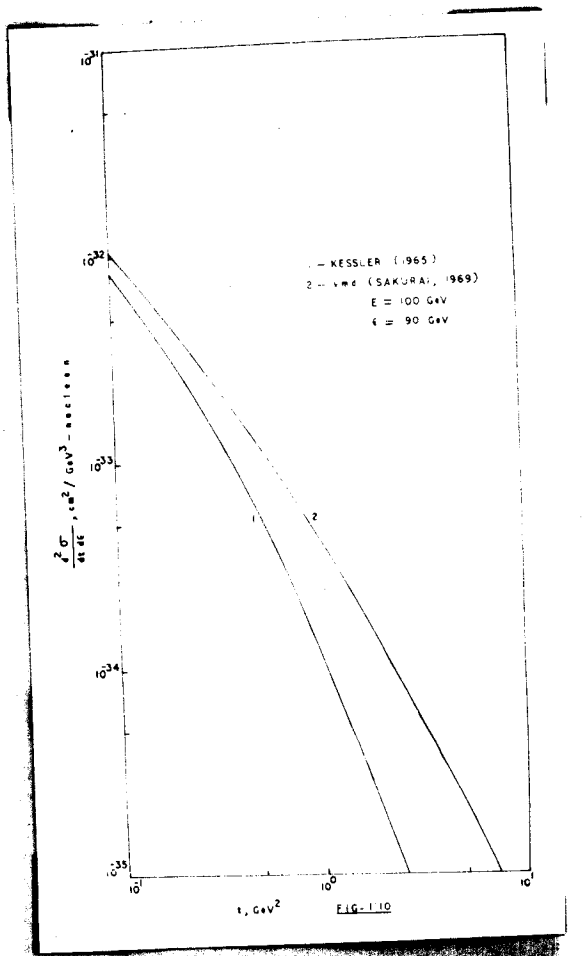

FIG-1.10

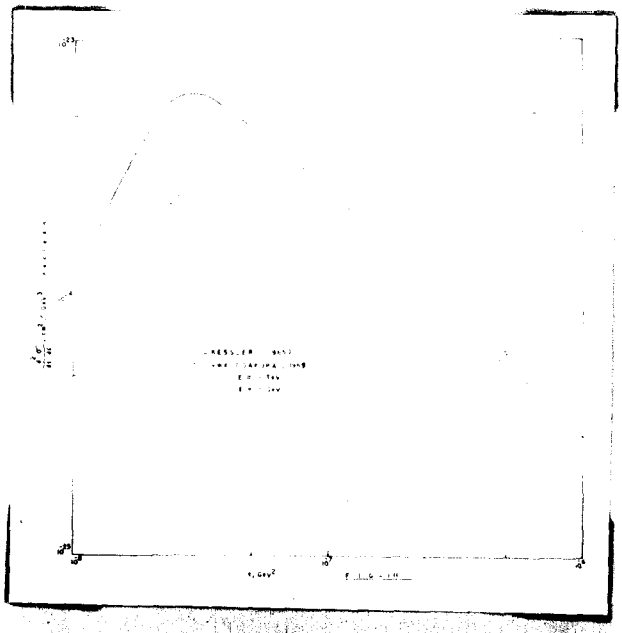

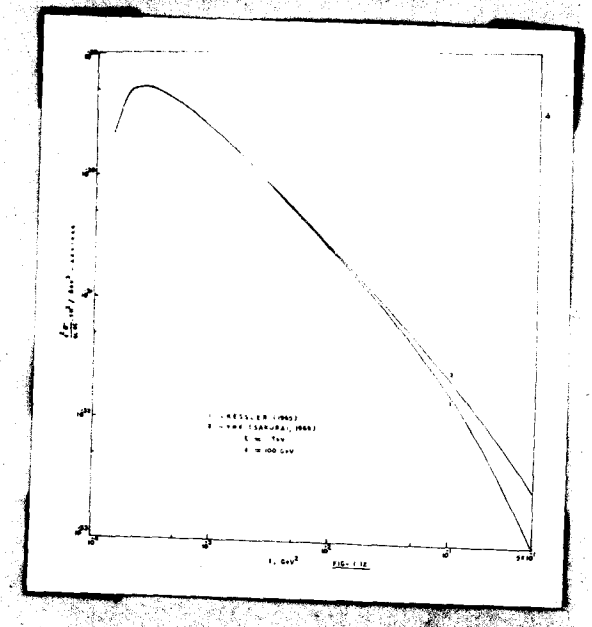

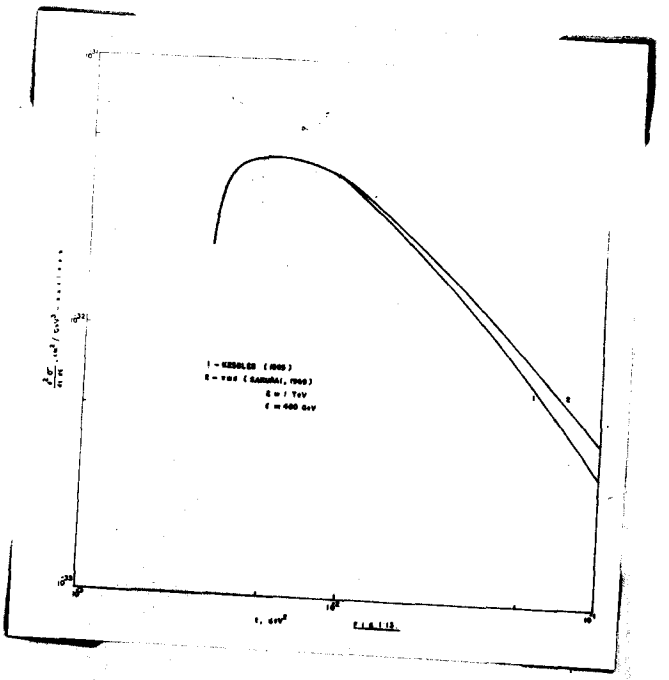

FIG. I.13

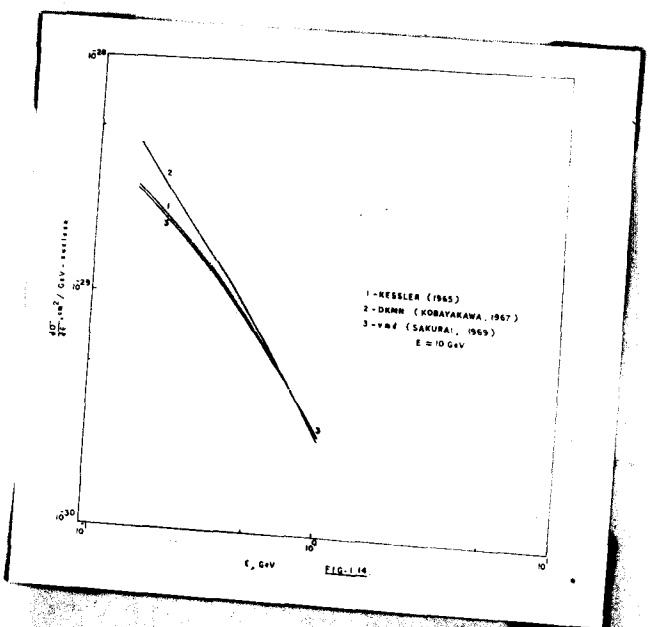

FIG. I.14

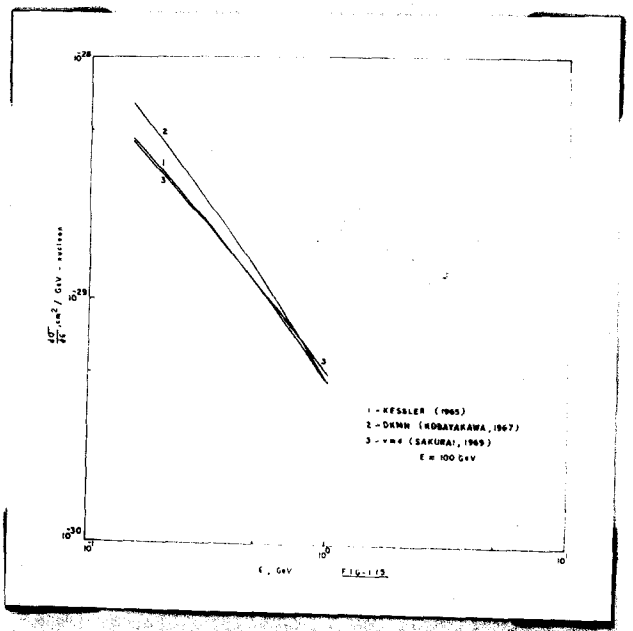

FIG-1 15

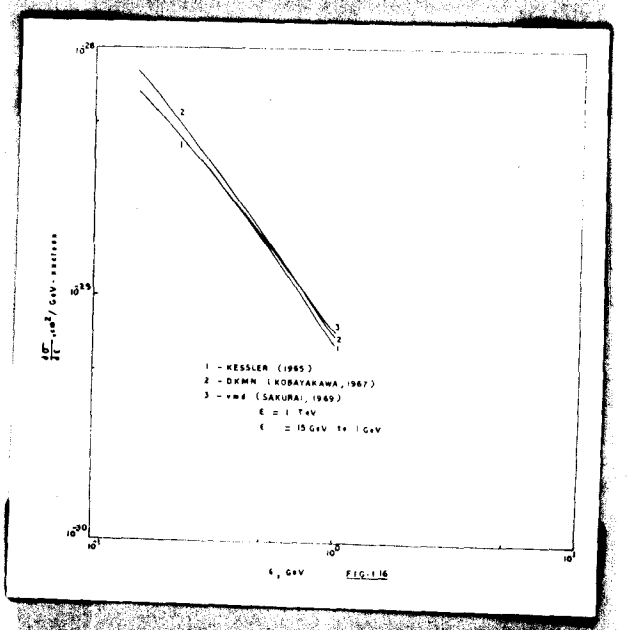

FIG-1 16

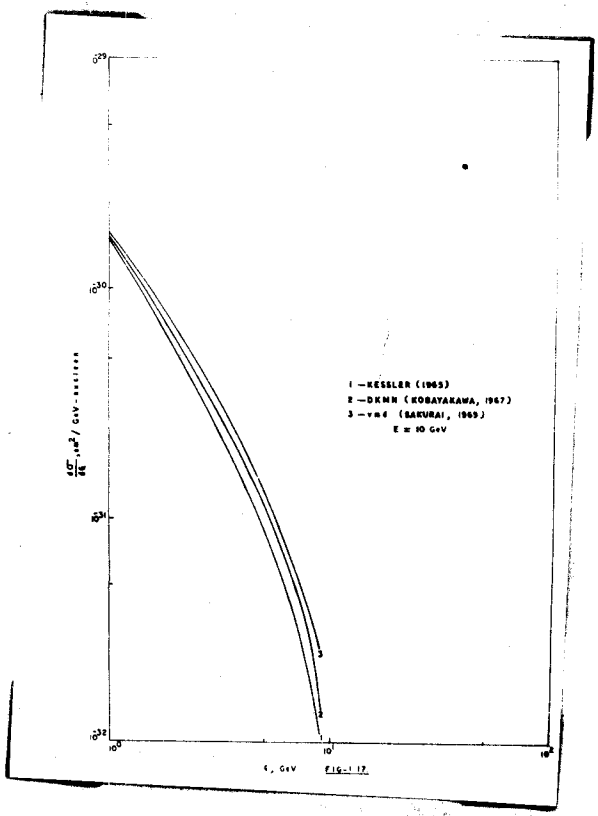

FIG- I 17

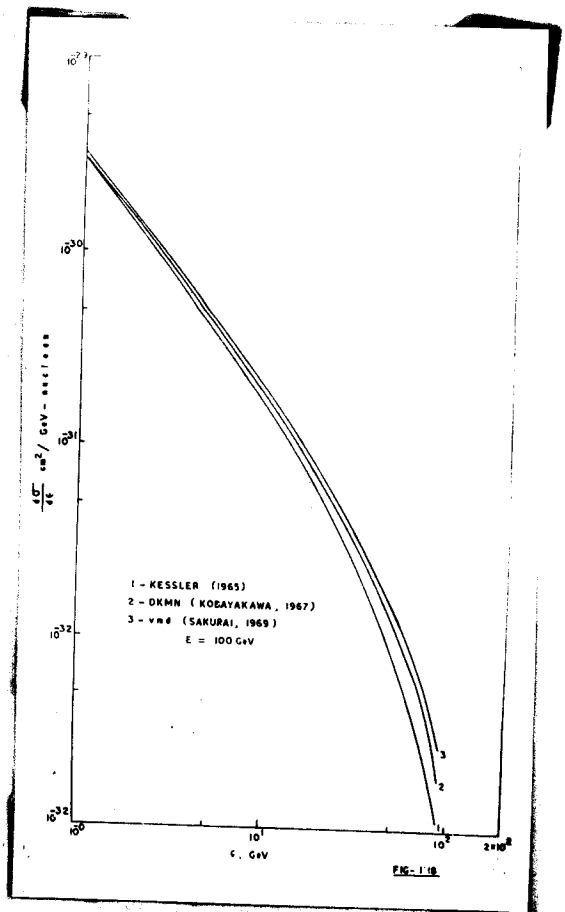

FIG- I 18

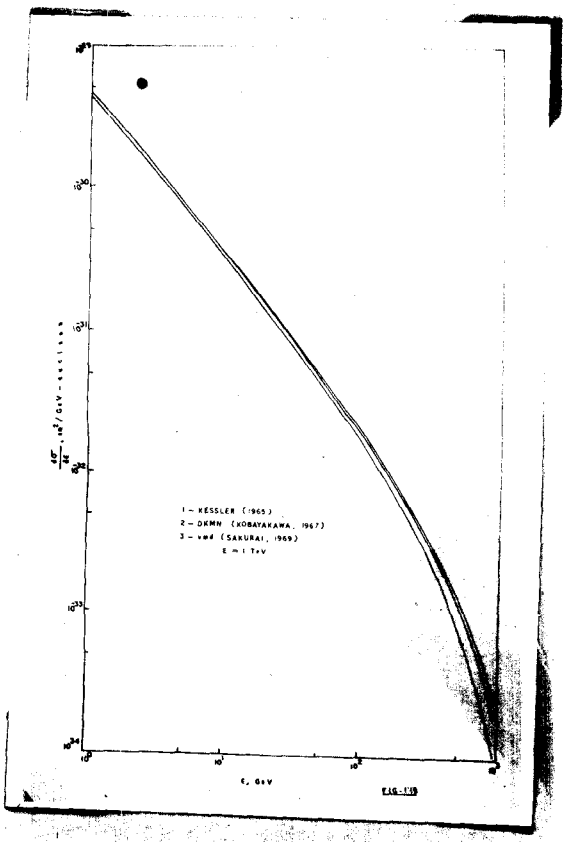

FIG. 1.19

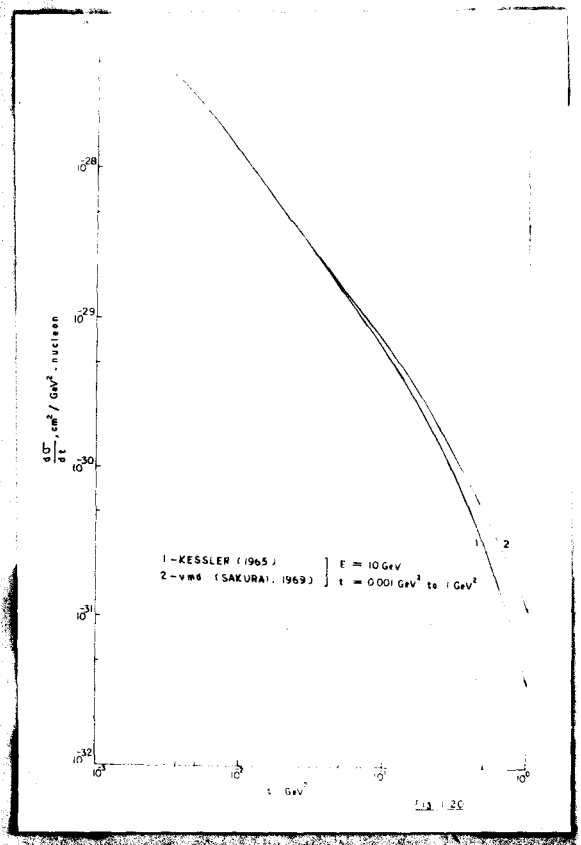

FIG. 1.20

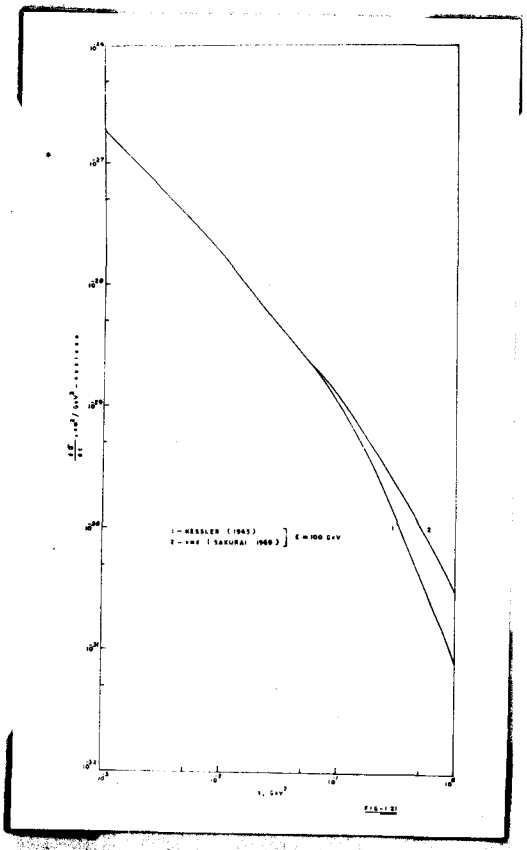
1 – KESSLER (1965)
2 – vmd (SAKURAI 1969)
E = 100 GeV
1
2
t, GeV²

FIG. 1.21

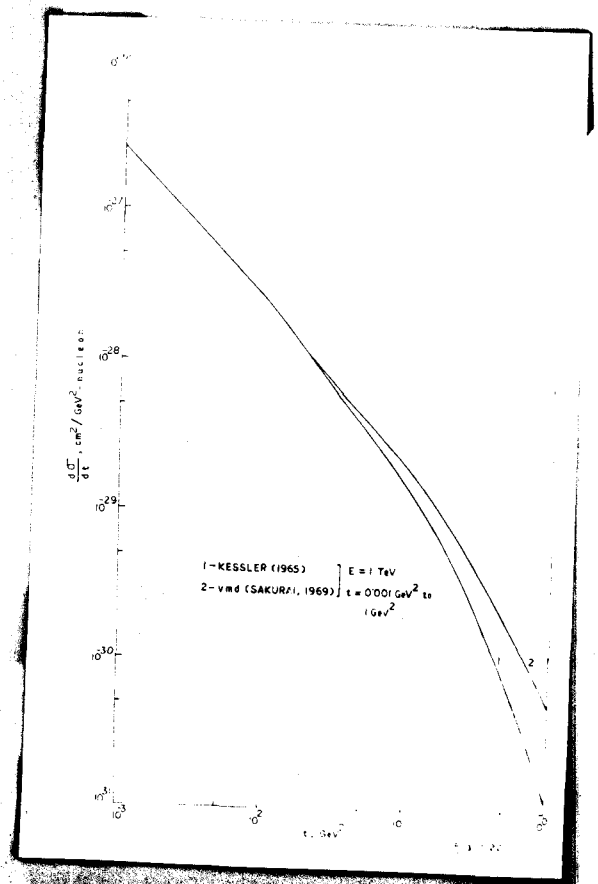
1 – KESSLER (1965)
2 – vmd (SAKURAI, 1969)
E = 1 TeV
t = 0.001 GeV² to 1 GeV²
dσ/dt, cm²/GeV² nucleon
t, GeV²
1
2

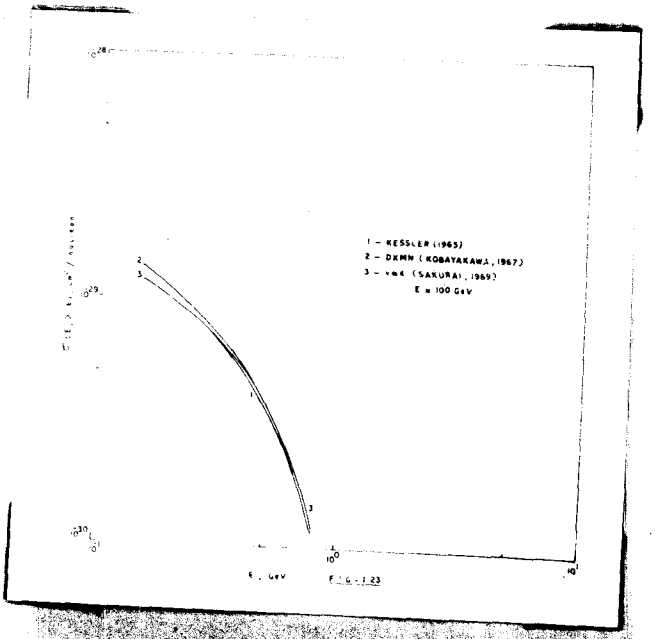

FIG. I.23

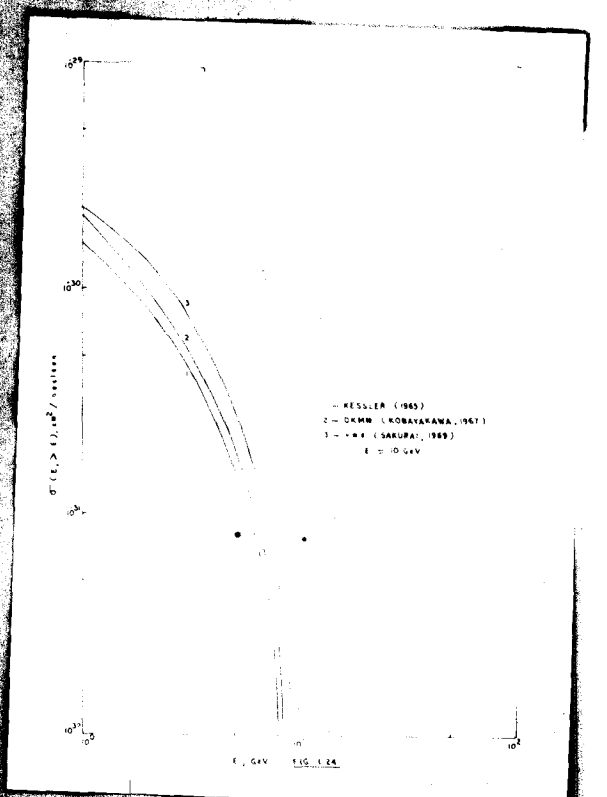

FIG. I.24

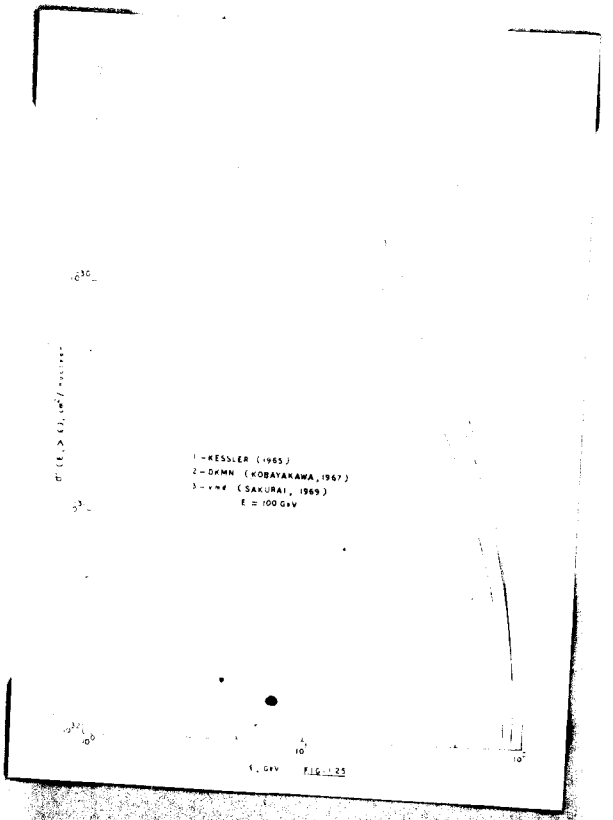

FIG - I 25

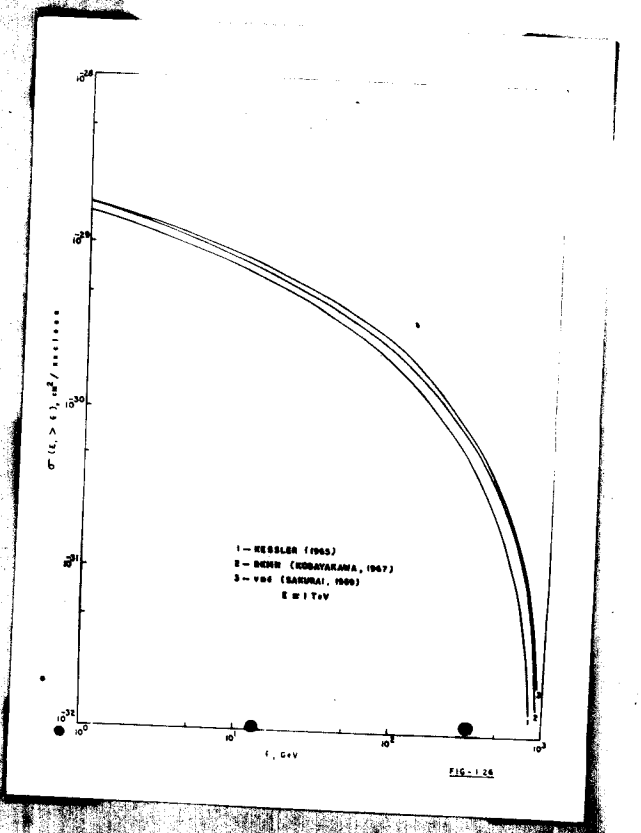

FIG - I 24

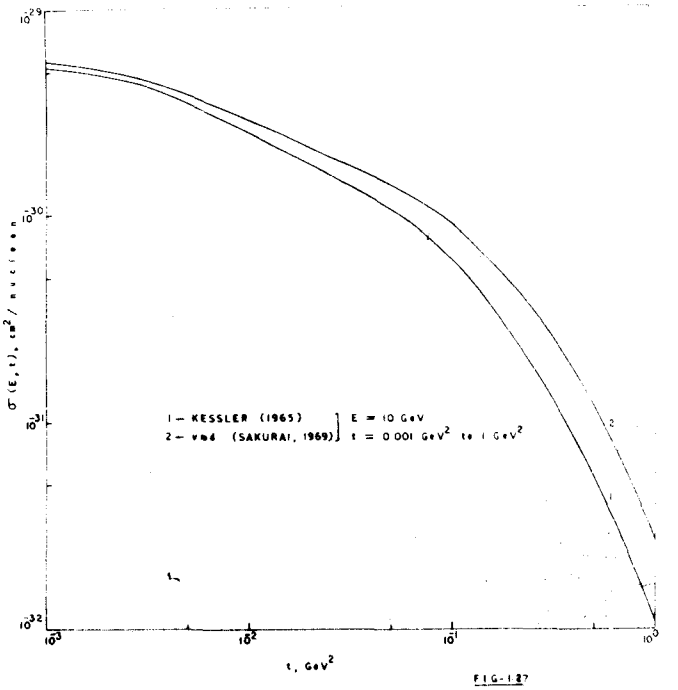

FIG-I.27

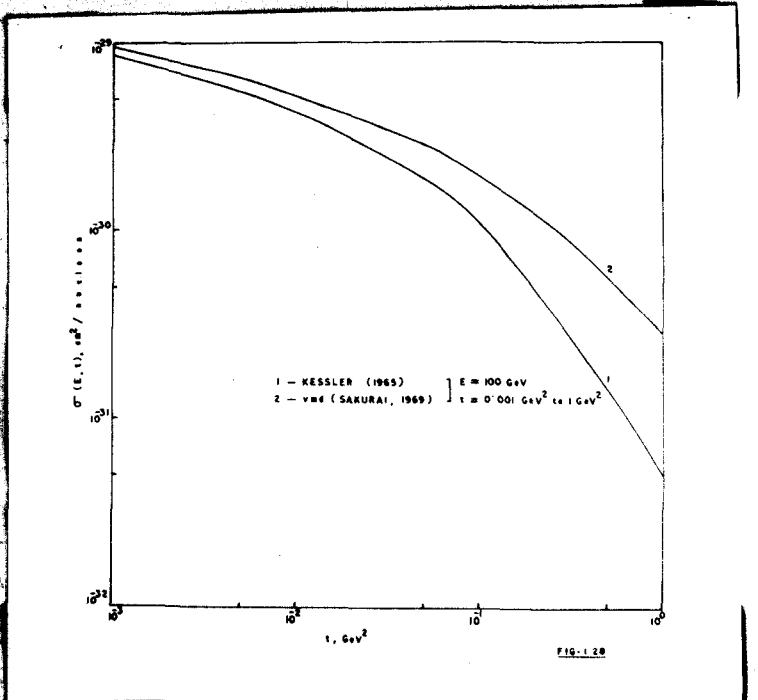

FIG-I.28

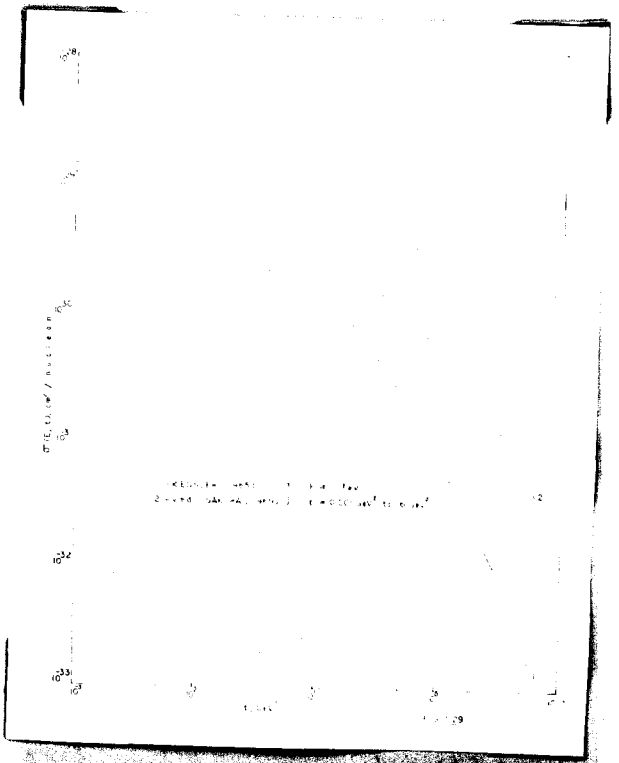

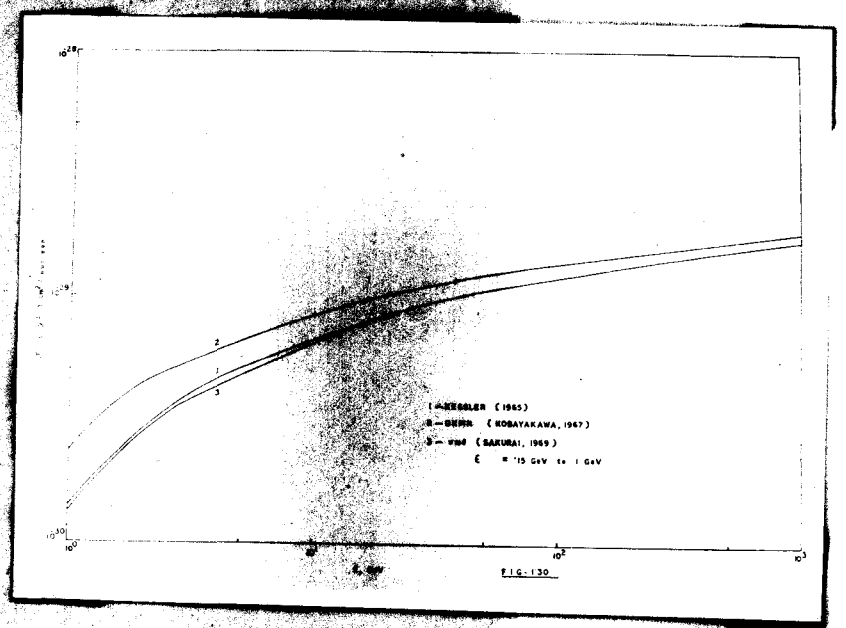
1—KESSLER (1965)
2—BERR (KOBAYAKAWA, 1967)
3— THIS (SAKURAI, 1969)
E = 15 GeV to 1 GeV

FIG-130

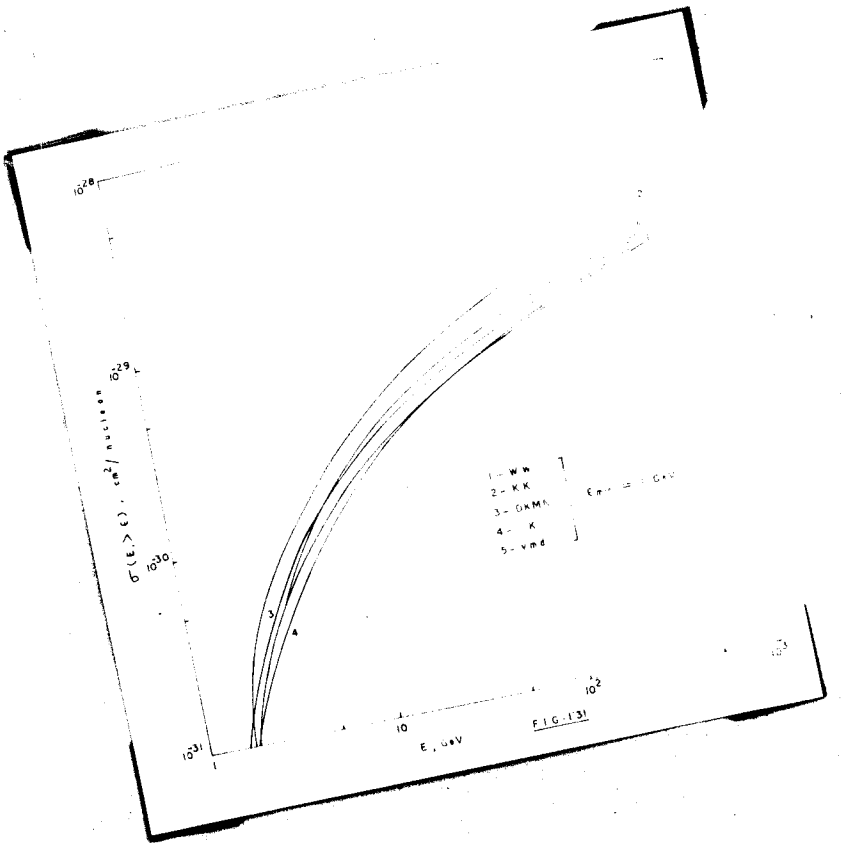

FIG-131

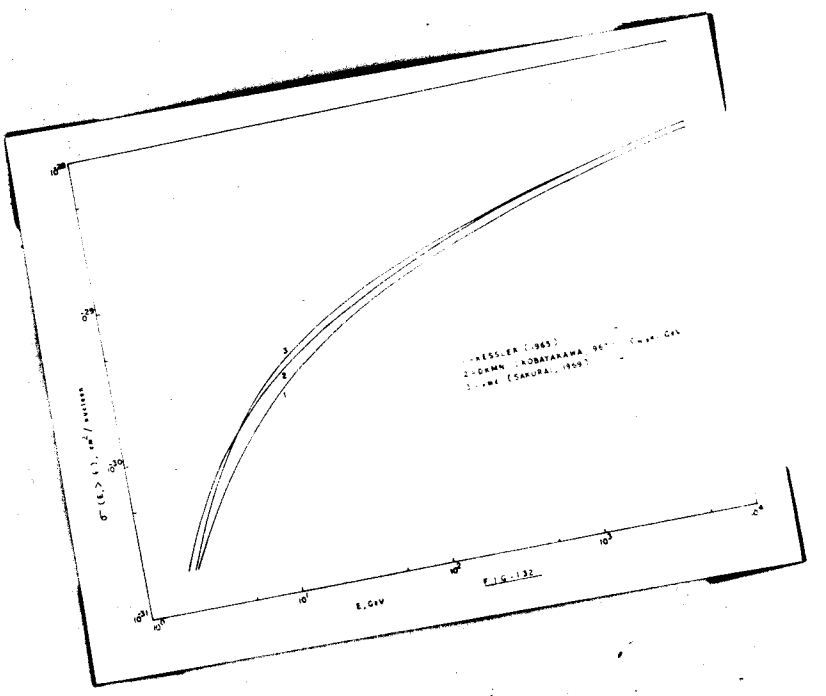

FIG-132

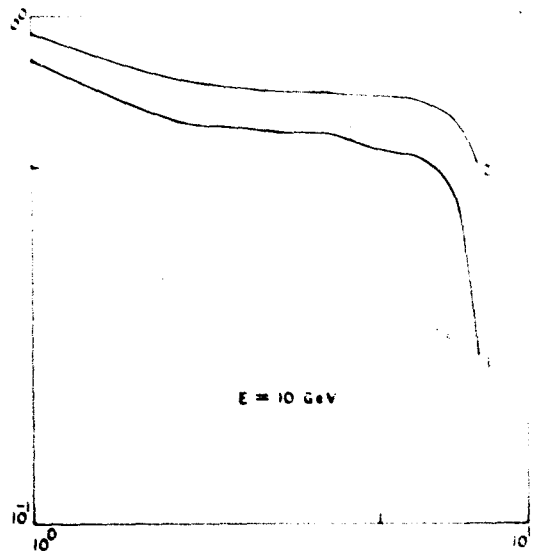

FIG-1.33 RATIO R OF INTEGRAL CROSS SECTIONS RELATIVE TO THE PREDICTED VALUE OF ν_{md} (SAKURAI), 1 – KESSLER / ν_{md}, 2 – DKMN / ν_{md}

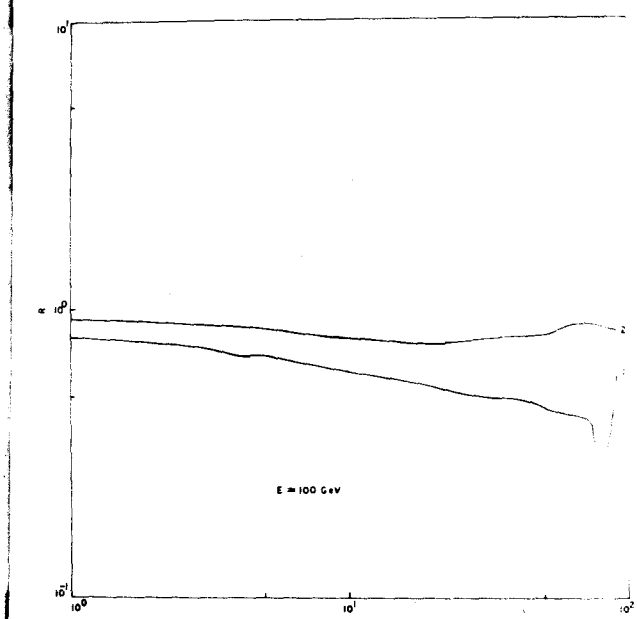

FIG-1.34 RATIO R OF INTEGRAL CROSS SECTIONS RELATIVE TO THE PREDICTED VALUE OF ν_{md} (SAKURAI) 1 – KESSLER / ν_{md}, 2 – DKMN / ν_{md}

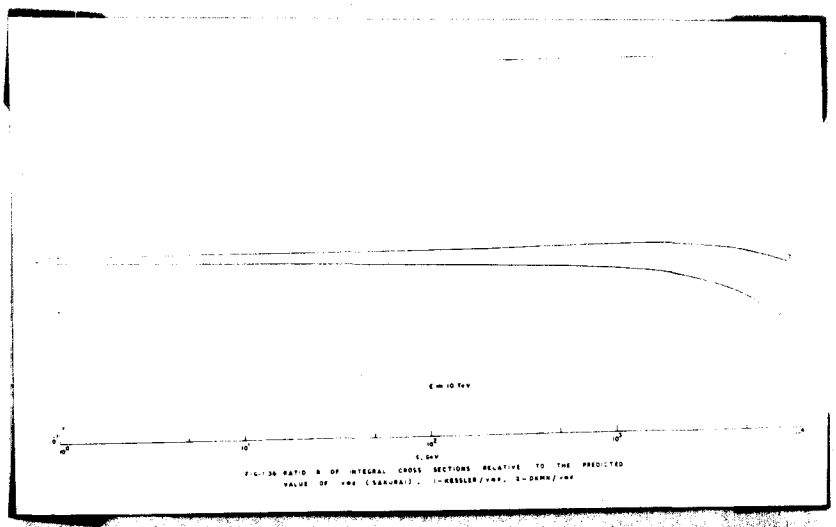

FIG. 36 RATIO R OF INTEGRAL CROSS SECTIONS RELATIVE TO THE PREDICTED VALUE OF $\nu_{\mu\mu}$ (SAKURAI). 1-KESSLER / $\nu_{\mu\mu}$, 2-OKMN / $\nu_{\mu\mu}$

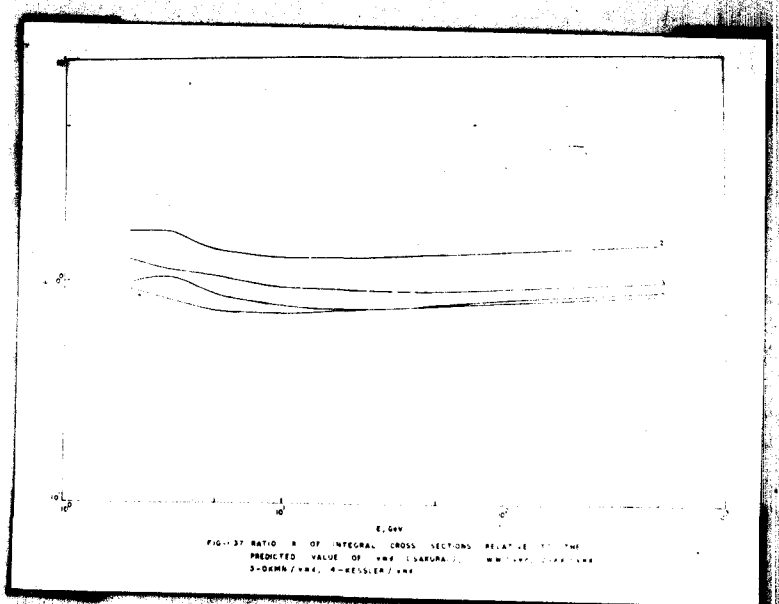

FIG. 37 RATIO R OF INTEGRAL CROSS SECTIONS RELATIVE TO THE PREDICTED VALUE OF $\nu_{\mu\mu}$ (SAKURAI). 3-OKMN / $\nu_{\mu\mu}$, 4-KESSLER / $\nu_{\mu\mu}$

Table 1.1 Computed values of differential cross sections for some values of ϵ at E = 10GeV

ϵ = 0.15 GeV

t GeV^2	$d^2\sigma/dKdt$, $10^3\mu b$ per GeV^3 - nucleon vmd model (Sakurai)	$d^2\sigma/d\epsilon dt$, $10^3\mu b$ per GeV^3 - nucleon (Kessler)
2.6×10^{-6}	257	257
3×10^{-6}	315	315
4×10^{-6}	390	390
5×10^{-6}	402	402
6×10^{-6}	398	398
10^{-5}	308	308
2×10^{-5}	178	178
3×10^{-5}	126	126
4×10^{-5}	97.50	97.50
6×10^{-5}	67	67
8×10^{-5}	50.80	50.80
10^{-4}	40.20	40.20
2×10^{-4}	20	20
3×10^{-4}	13.50	13.50
4×10^{-4}	10.10	10.10
6×10^{-4}	6.70	6.70
8×10^{-4}	5	5
10^{-3}	3.92	4
2×10^{-3}	1.86	1.98

Table 1.1 (contd.)

ϵ = 0.15 GeV

t GeV^2	$d^2\sigma/dk\,dt$, $10^3\mu$b per GeV^3-nucleon vmd model (Sakurai)	$d^2\sigma/d\epsilon\,dk$ $10^3\mu$b per GeV^3 - nucleon (Kessler)
3 x 10^3	1.20	1.28
4 x 10^3	0.86	0.93
5 x 10^{-3}	0.66	0.73
6 x 10^{-3}	0.53	0.59
8 x 10^{-3}	0.38	0.43
10^{-2}	0.28	0.33

Table 1.1 (contd.)

ϵ = 38eV

t GeV^2	$d^2\sigma/dk\,dt$, $10^{-2}\mu$ b per GeV^3- nucleon vmd model (Sakurai)	$d^2\sigma/d\epsilon\,dt$, $10^{-2}\mu$ b per GeV^3- nucleon (Kessler)
10^{-2}	611	589
1.5 x 10^{-2}	438	400
2 x 10^{-2}	332	300
3 x 10^{-2}	224	195
4 x 10^{-2}	167	140
5 x 10^{-2}	131	108
6 x 10^{-2}	107	86
7 x 10^{-2}	89	70.20
8 x 10^{-2}	76.50	59.00
9 x 10^{-2}	66.50	50.50
10^{-1}	58.60	43.60
1.5 x 10^{-1}	35	24
2 x 10^{-1}	25.90	15
3 x 10^{-1}	13.30	7.30
4 x 10^{-1}	8.75	4.20
5 x 10^{-1}	6.20	2.65
6 x 10^{-1}	4.65	1.78
7 x 10^{-1}	3.60	1.26
8 x 10^{-1}	2.90	0.93
9 x 10^{-1}	2.38	0.70
10^{0}	1.93	0.55

Table 1.1 (contd.)

ϵ = 9 GeV

t GeV^2	$d^2\sigma/dk\,dt$, $10^{-3}\mu b$ per GeV^3- nucleon vmd model (Sakurai)	$d^2\sigma/d\epsilon\,dt$, $10^{-3}\mu b$ per GeV^3- nucleon (Kessler)
10^{-1}	113	82.40
1.5×10^{-1}	74	47.10
2×10^{-1}	55	30.30
2.5×10^{-1}	40.50	19.70
3×10^{-1}	32.50	15.40
4×10^{-1}	22	8.90
5×10^{-1}	16	5.70
6×10^{-1}	1.22	3.85
7×10^{-1}	9.65	2.70
8×10^{-1}	7.80	1.98
9×10^{-1}	6.45	1.50
10^{0}	5.35	1.14

Table 1.2 Computed values of differential cross sections for some values of ϵ at E = 100 GeV

ϵ = 0.30 GeV

t Gev^2	$d^2\sigma/dk\,dt$, $10^3\mu b$ per GeV^3 - nucleon vmd model (Sakurai)	$d^2\sigma/d\epsilon\,dt$, $10^3\mu b$ per GeV^3 - nucleon (Kessler)
1.2×10^{-7}	2550	2550
1.5×10^{-7}	3100	3100
2×10^{-7}	3950	3950
2.5×10^{-7}	4400	4400
3×10^{-7}	4380	4380
3.5×10^{-7}	4100	4100
4×10^{-7}	3790	3790
5×10^{-7}	3150	3150
6×10^{-7}	2700	2700
7×10^{-7}	2360	2360
8×10^{-7}	2100	2100
9×10^{-7}	1900	1900
10^{-6}	1740	1740
2×10^{-6}	920	920
3×10^{-6}	623	623
4×10^{-6}	475	475
6×10^{-6}	320	320
8×10^{-6}	240	240
10^{-5}	190	190

Table 1.2 (contd.)

ϵ = 0.308eV

t GeV^2	$d^2\sigma/dk\,dt$, $10^3\mu b$ per GeV^{-2} nucleon vmd model (Sakurai)	$d^2\sigma/d\epsilon\,dt$, $10^3\mu b$ per GeV^{-3} nucleon (Kessler)
2×10^{-5}	95	95
3×10^{-5}	64	64
5×10^{-5}	38	38
8×10^{-5}	23.80	23.80
10^{-4}	19.00	19.00
2×10^{-4}	9.50	9.50
3×10^{-4}	6.40	6.40
5×10^{-4}	3.80	3.80
8×10^{-4}	3.40	3.40
10^{-3}	1.91	1.91

Table 1.2 (contd.)

ϵ = 20 GeV

t GeV^2	$d^2\sigma/dkdt$, μb per GeV^3 - nucleon vmd model (Sakurai)	$d^2\sigma/d\epsilon dt$, μb per GeV^3 - nucleon (Kessler)
10^{-3}	5.38	5.38
1.5×10^{-3}	4.68	4.68
2×10^{-3}	4.05	4.05
2.5×10^{-3}	3.58	3.58
3×10^{-3}	3.23	3.23
3.5×10^{-3}	2.83	2.79
4×10^{-3}	3.52	3.47
5×10^{-3}	2.10	2.05
6×10^{-3}	1.78	1.63
7×10^{-3}	1.55	1.50
8×10^{-3}	1.38	1.33
10^{-2}	1.11	1.07
1.5×10^{-2}	0.75	0.71
2×10^{-2}	0.57	0.52
3×10^{-2}	0.37	0.33
4×10^{-2}	0.27	0.24
5×10^{-2}	0.22	0.18
6×10^{-2}	0.18	0.14
7×10^{-2}	0.15	0.012
8×10^{-2}	0.13	0.010
9×10^{-2}	0.11	0.009
10^{-1}	0.10	0.007

Table 1.2 (Contd.)

ϵ = 90 GeV

t GeV^2	$d^2\sigma/dk\,dt$, $10^{-3}\mu b$ per GeV^3- nucleon vmd model (Sakurai)	$d^2\sigma/d\epsilon\,dt$, $10^{-3}\mu b$ per GeV^3- nucleon (Kessler)
10^{-1}	11.20	8.15
1.5 x 10^{-1}	6.47	4.70
2 x 10^{-1}	4.48	3.03
3 x 10^{-1}	2.60	1.54
4 x 10^{-1}	1.73	0.92
5 x 10^{-1}	1.23	0.59
6 x 10^{-1}	0.95	0.40
7 x10 $^{-1}$	0.75	0.27
8 x 10^{-1}	0.60	0.20
9 x 10 $^{-1}$	0.50	0.15
10^{0}	0.41	0.12
1.5	0.21	0.04
2	0.12	0.02
2.5	0.08	0.01

Table 1.3 Calculated values of differential cross sections for some values of ϵ at E = 1 TeV

= 1 GeV

t GeV^2	$d^2\sigma/dk\,dt$, $10^3\mu b$ per GeV^3- nucleon vmd model (Sakurai)	$d^2\sigma/d\epsilon\,dt$, $10^3\mu b$ per GeV^3- nucleon (Kessler)
1.2 x 10^{-8}	1630	1630
1.4 x 10^{-8}	2340	2340
1.6 x 10^{-8}	3050	3050
1.8 x 10^{-8}	3750	3750
2 x 10^{-8}	4340	4340
2.3 x 10^{-8}	5420	5420
2.5 x 10^{-8}	5820	5820
3 x 10^{-8}	6060	6060
3.5 x 10^{-8}	5800	5800
4 x 10^{-8}	5280	5280
5 x 10^{-8}	4500	4500
6 x10^{-8}	3900	3900
7 x 10^{-8}	3460	3460
8 x 10^{-8}	3100	3100
9 x 10^{-8}	2810	2810
10^{-7}	2580	2580
1.5 x 10^{-7}	1780	1780
2 x 10^{-7}	1370	1370
2.5 x 10^{-7}	1110	1110
3 x 10^{-7}	929	929
4 x10^{-7}	710	710
5 x 10^{-7}	575	575
6 x 10^{-7}	480	480
7 x 10^{-7}	412	412
8 x 10^{-7}	362	362
9 x 10^{-7}	322	322
10^{-6}	288	288

Table 1.3 (contd.)

ϵ = 100 GeV

t GeV^2	$d^2\sigma/dk\,dt$, 10^{-3} μb per GeV^3 - nucleon vmd model (Sakurai)	$d^2\sigma/d\epsilon\,dt$, 10^{-3} μb per GeV^3 - nucleon (Kessler)
1.4×10^{-4}	2180	2180
1.7×10^{-4}	3800	3800
2×10^{-4}	5010	5010
2.5×10^{-4}	5200	5200
3×10^{-4}	5150	5150
3.5×10^{-4}	4800	4800
4×10^{-4}	4450	4450
5×10^{-4}	3950	3950
6×10^{-4}	3450	3450
7×10^{-4}	3080	3080
8×10^{-4}	2760	2760
9×10^{-4}	2510	2510
10^{-3}	2300	2300
2×10^{-3}	1240	1240
3×10^{-3}	829	829
5×10^{-3}	500	495
8×10^{-3}	320	305
10^{-2}	256	246
2×10^{-2}	128	118
3×10^{-2}	82.90	74.80
5×10^{-2}	48	40.90
8×10^{-2}	28.20	12.20
10^{-1}	22.30	16.30
1.5×10^{-1}	13.60	8.90
2×10^{-1}	8.90	5.48
3×10^{-1}	5.73	2.64
4×10^{-1}	3.80	1.52
5×10^{-1}	2.78	1.00

Table 1.3 (contd.)

ϵ = 400 GeV

t GeV^2	$d^2\sigma/dk\,dt$, 10^{-3} mb per GeV^3 -nucleon vmd model (Sakurai)	$d^2\sigma/d\epsilon\,dt$, 10^{-3} mb per GeV^3 nucleon (Kessler)
3 x 10^{-3}	20	20
3.2 x 10^{-3}	30	30
3.5 x 10^{-3}	37.60	37.60
4 x 10^{-3}	41.70	41.70
4.5 x 10^{-3}	42.60	42.60
5 x 10^{-3}	43	43
5.5 x 10^{-3}	43	43
6 x 10^{-3}	42.80	42.80
7 x 10^{-3}	11.20	11.20
8 x 10^{-3}	39.90	39.90
9 x 10^{-3}	37.90	37.00
10^{-2}	35.90	34.50
1.5 x 10^{-2}	25.90	24.70
2 x 10^{-2}	20.20	19
3 x 10^{-2}	14.10	12.70
4 x 10^{-2}	10.70	9.35
5 x 10^{-2}	8.37	7.25
6 x 10^{-2}	7	5.82
7 x 10^{-2}	6	4.81
8 x 10^{-2}	5.20	4.05
9 x 10^{-2}	4.58	3.90
10^{-1}	4.08	2.98

Table 1.4 Computed values of differential cross sections for different values of ϵ, at E = 10 GeV

Transfer energy GeV	$\frac{d\sigma}{d\epsilon}$, μb per GeV-nucleon vmd model(Sakurai)	$\frac{d\sigma}{d\epsilon}$, μb per GeV-nucleon DESY (Kobayakawa)	(Kessler)
0.15	27.80	45	28.40
0.18	24	34.30	24.60
0.20	21	28.60	21.60
0.25	16.80	20.90	17.20
0.30	13.80	16.40	14
0.35	11.90	13.20	11.80
0.40	9.70	11.10	10
0.45	8.38	9.35	8.60
0.50	7.25	7.97	7.42
0.60	5.65	6	5.73
0.70	4.54	4.68	4.55
0.80	3.71	3.68	3.68
0.90	3.10	3	3
1	2.64	2.50	2.50

Table 1.5 Computed values of differential cross sections for different values of ϵ, at E = 100 GeV

Transfer energy GeV	$\frac{d\sigma}{d\epsilon}$, μb per GeV - nucleon	$\frac{d\sigma}{d\epsilon}$, μb per GeV-nucleon	
	vmd model(Sakurai)	DESY (Kobayakawa)	(Kessler)
0.15	45.90	62.80	46.70
0.18	38.40	53.50	39.20
0.20	33.30	45.90	33.80
0.23	29.30	39	29.70
0.25	26.10	34.20	26.50
0.30	22.60	27	23
0.35	18	21.90	18
0.40	15.20	18	15.20
0.45	13.30	15.40	13.20
0.50	11.70	13.20	11.90
0.60	9.45	10.10	9.20
0.70	7.82	8	7.48
0.80	6.62	6.60	6.25
0.90	5.70	5.42	5.34
1	4.95	4.60	4.60

Table 1.6 Computed values of differential cross sections for different values of ϵ, at E = 1 TeV

Transfer energy GeV	$\frac{d\sigma}{d\epsilon}$, μb per GeV - nucleon, vmd model(Sakurai)	$\frac{d\sigma}{d\epsilon}$, μb per GeV-nucleon DKMH (Kobayakawa)	(Kessler)
0.15	66.70	80.70	66.70
0.10	57.10	67.30	57.10
0.20	49.80	57	49.80
0.25	39	43.90	39
0.30	31.50	34.60	31.80
0.35	26.90	28.90	26.40
0.40	22.20	23.90	21.90
0.45	19.90	20.90	19.20
0.50	17.20	17.80	16.70
0.60	13.70	14	13
0.70	11.20	11.20	10.80
0.80	9.40	9.40	8.80
0.90	8.12	8	7.40
1	7.14	6.90	6.38

Table 1.7 Computed values of differential cross sections for different values of ϵ at E = 100eV

Transfer energy GeV	$\frac{d\sigma}{d\epsilon}$, $10^{-3}\mu b$ per Gev - nucleon, vmd model(Sakurai)	$\frac{d\sigma}{d\epsilon}$, $10^{-3}\mu b$ per GeV-nucleon, DRMF (Kobayakawa)	(Kessler)
1	1790	1680	1630
1.5	1020	938	860
2	665	595	525
2.5	468	410	352
3	350	299	249
3.5	261	228	175
4	202	178	141
4.5	160	138	110
5	127	110	85.50
6	85	72.40	55.70
7	56.20	46.50	34
8	38.20	31.70	20
9	26.50	13.80	11

Table 1.8 Computed values of differential cross sections for different values of ϵ at E = 100 GeV

Transfer energy Gev	$\frac{d\sigma}{d\epsilon}$, $10^{-3}\mu$b per GeV-nucleon vmd model(Sakurai)	$\frac{d\sigma}{d\epsilon}$, $10^{-3}\mu$b per GeV-nucleon DESY (Kobayakawa)	(Kessler)
1	3210	3000	3010
1.5	2020	1900	1820
2	1440	1390	1290
2.5	1110	1040	970
3	881	840	769
4	620	585	530
5	470	440	398
6	372	342	312
7	305	281	252
8	255	235	211
9	220	200	180
10	189	174	155
15	108	97	84
20	69.90	62.10	52.70
25	48.70	43.80	35.40
30	36	32.20	25
40	21.60	18.60	13.90
50	14.20	11.80	7.97
60	9.70	7.93	4.82
70	6.68	5.19	3
80	4.40	3.50	1.84
90	2.70	1.81	1.10

Table 1.9 Computed values of differential cross sections for different values of ϵ at E = 1TeV

Transfer energy GeV	$\frac{d\sigma}{d\epsilon}$, $10^{-3}\mu b$ per GeV-nucleon vmd model(Sakurai)	$\frac{d\sigma}{d\epsilon}$, $10^{-3}\mu b$ per GeV-nucleon DKSW (KOBAYAKAWA)	(KESSLER)
1	4570	4570	4180
1.5	3000	3000	2720
2	2180	2180	2000
2.5	1680	1680	1530
3	1330	1330	1230
4	965	965	895
5	741	741	690
7	497	497	465
10	326	324	300
15	208	202	183
20	147	142	129
25	113	110	100
30	91	88	80
40	63.30	60.70	56
50	48	45.8	42
60	38	36	33
80	26.50	24.50	22.50
100	19.40	18	16
150	10.80	10	8.90
200	6.90	6.50	5.42
250	4.81	4.58	3.70
300	3.55	3.32	2.65
400	2.15	2	1.46
500	1.38	1.27	0.82
600	0.88	0.78	0.49
700	0.60	0.50	0.30
800	0.42	0.33	0.19
900	0.29	0.22	0.11

Table 1.10 Computed values of differential cross sections for different values of t at E = 10 GeV

t GeV^2	$\frac{d\sigma}{dt}$, μb per GeV^2 nucleon	
	V M D model (Sakurai)	(Kessler)
10^{-3}	968	968
1.5×10^{-3}	760	760
2×10^{-3}	627	627
2.5×10^{-3}	540	540
3×10^{-3}	470	470
4×10^{-3}	360	360
5×10^{-3}	285	285
6×10^{-3}	233	233
7×10^{-3}	197	197
8×10^{-3}	167	167
9×10^{-3}	144	144
10^{-2}	128	128
1.5×10^{-2}	74	74
2×10^{-2}	50.30	50.30
3×10^{-2}	40	39.80
4×10^{-2}	20.90	20.30
5×10^{-2}	15.80	15.20
6×10^{-2}	12.80	11.90
8×10^{-2}	9.10	8.15
10^{-1}	7.14	6.13
1.5×10^{-1}	3.86	3.24
2×10^{-1}	2.90	2
3×10^{-1}	1.26	0.92
4×10^{-1}	0.75	0.49
5×10^{-1}	0.49	0.29
6×10^{-1}	0.34	0.17
8×10^{-1}	0.19	0.08
10^{0}	0.12	0.04

Table 1.11 Computed values of differential cross sections for different values of t at E = 100 GeV

t GeV^2	$\frac{d\sigma}{dt}$, μb per GeV^2 - nucleon	
	vmd model (Sakurai)	(Kessler)
10^{-3}	1890	1890
1.5 x10^{-3}	1250	1250
2 x10^{-3}	920	920
3 x10^{-3}	614	614
3.5 x10^{-3}	520	520
4 x 10^{-3}	453	453
5 x 10^{-3}	360	360
6 x 10^{-3}	300	300
8 x 10^{-3}	222	222
10^{-2}	191	191
2 x 10^{-2}	76	76
3 x,10^{-2}	47	47
4 x 10^{-2}	34.20	34.20
5 x 10^{-2}	26.90	26.90
6 x 10^{-2}	21.80	21.60
7 x 10^{-2}	18.90	17.80
8 x 10^{-2}	16.20	15
9 x 10^{-2}	14.20	12.70
10^{-1}	12.70	11.20
1.5 x 10^{-1}	7.10	5.68
2 x 10^{-1}	4.63	3.20
2.5 x 10^{-1}	2.90	2
3 x 10^{-1}	2.53	1.28
4 x 10^{-1}	1.56	0.68
5 x 10^{-1}	1.08	0.41
6 x 10^{-1}	0.79	0.27
8 x 10^{-1}	0.48	0.14
10^{0}	0.32	0.08

Table 1.12 Computed values of differential cross sections for different values of t at E = 1 TeV

t GeV^2	$\frac{d\sigma}{dt}$, μb per GeV^2 nucleon	
	vmd model (Sakurai)	(Kessler)
10^{-3}	2500	2500
1.5×10^{-3}	1670	1670
2×10^{-3}	1260	1260
3×10^{-3}	840	840
4×10^{-3}	630	630
6×10^{-3}	420	420
8×10^{-3}	315	315
10^{-2}	253	253
1.5×10^{-2}	152	152
2×10^{-2}	109	107
2.5×10^{-2}	84	81
3×10^{-2}	67.30	63.90
4×10^{-2}	50	44.90
5×10^{-2}	39.50	34
6×10^{-2}	32.50	27
9×10^{-2}	21.50	16.60
10^{-1}	19.70	14.30
1.5×10^{-1}	11.20	7 .80
2×10^{-1}	7.58	4.70
2.5×10^{-1}	5.40	3.10
3×10^{-1}	4.01	2.11
4×10^{-1}	2.55	1.15
5×10^{-1}	1.76	0.71
6×10^{-1}	1.30	0.46
7×10^{-1}	1	0.31
8×10^{-1}	0.78	0.22
9×10^{-1}	0.62	0.16
10^{0}	0.52	0.12

Table 1.13 Computed values of integral cross sections for different values of ϵ at E = 100 GeV

Transfer energy GeV	σ, mb per nucleon		
	vmd model (Sakurai)	DKMM (Kobayakawa)	(Kessler)
0.15	11.90	13.60	11.90
0.175	10.80	12.10	10.80
0.20	10	11.10	10
0.25	8.40	9	8.40
0.30	7.20	7.52	7.04
0.35	6.06	6.40	6
0.40	5.25	5.40	5.05
0.45	4.50	4.50	4.25
0.50	3.81	3.81	3.65
0.60	2.68	2.65	2.52
0.70	1.85	1.75	1.75
0.80	1.25	1.15	1.15

Table 1.14 Computed values of integral cross sections for different values of ϵ at E = 10 GeV

Transfer energy, GeV	σ, $10^{-3}\mu b$ per nucleon		
	vmd model (Sakurai)	DDMN (Kobayakawa)	(Kessler)
1	2250	2060	1780
1.5	1680	1350	1160
2	1300	959	814
2.5	990	712	600
3	771	540	456
3.5	595	413	349
4	462	322	265
4.5	362	250	203
5	288	196	155
6	172	115	89.90
7	98.80	62	46
8	50	25	11

Table 1.15 Computed values of integral cross sections for different values of ϵ at E = 100 GeV

Transfer energy, GeV	σ, $10^{-3}\mu$b per nucleon		
	VMD model (Sakurai)	DEMM (Kobayakawa)	(Kessler)
1	8640	7990	6950
1.5	7350	6850	5750
2	6550	5960	5010
2.5	5890	5360	4430
3	5410	4860	4000
3.5	5000	4480	3670
4	4700	4120	3380
5	4140	3560	2880
6	3750	3190	2530
7	3430	2860	2250
8	3180	2590	2010
9	2930	2370	1830
10	2730	2180	1670
15	1930	1500	1100
20	1430	1090	779
25	1090	825	560
30	824	648	415
35	630	497	315
40	483	388	238
50	294	238	134
60	170	143	79.50
70	95.50	84.30	42.30
80	47	42	15
90	12.80	10.70	7.55

Table 1.16 Computed values of integral cross sections for different values of ϵ at E = 1 TeV

Transfer energy GeV	σ, $10^{-1}\,\mu$b per nucleon		
	vmd model (Sakurai)	DKMM (Kobayakawa)	(Kessler)
1	175	175	154
1.5	156	153	137
2	145	142	128
2.5	135	131	118
3	129	123	111
4	118	112	101
5	108	104	92.50
6	102	97	87
7	97	91.50	82
8	93	87	78
10	84.90	79.50	71.60
15	71.80	66	59.50
20	63.60	59.40	52.90
25	56.60	51.80	46
30	51.80	47	42
40	44.30	40	35.10
50	39	35.60	30.90
60	31.50 35.00	35.00 31.50	27.00
80	29.00	25.00	21.80
100	24.90	22	18.50
150	16.90	15	12
200	12.90	11.20	8.65
300	7.18	6.50	4.70
400	4.40	4.08	2.75
500	2.80	2.60	1.60
600	1.72	1.61	0.92
700	1.04	0.97	0.46
800	0.58	0.52	0.20
900	0.21	0.14	0.07

Table 1.17 Computed values of integral cross sections for different values of t at E = 10 GeV

t GeV^2	σ, 10^{-3} μb per nucleon	
	V m.d model (Sakurai)	(Kegeler)
10^{-3}	3.62	3.28
1.5×10^{-3}	3.30	3
2×10^{-3}	3	2.73
2.5×10^{-3}	2.92	2.50
3×10^{-3}	2.65	2.31
4×10^{-3}	2.18	1.82
6×10^{-3}	1.62	1.27
8×10^{-3}	1.20	0.80
10^{-2}	0.91	0.56
1.5×10^{-2}	0.41	0.02
2×10^{-2}	0.10	0.75
3×10^{-2}	0.78	0.43
4×10^{-2}	0.53	0.20
5×10^{-2}	0.39	0.06
6×10^{-2}	0.29	0.96
7×10^{-2}	0.14	0.85
8×10^{-2}	0.05	0.76
9×10^{-2}	0.98	0.69
10^{-1}	0.92	0.63
1.5×10^{-1}	0.62	0.38
2×10^{-1}	0.46	0.26
2.5×10^{-1}	0.35	0.19
3×10^{-1}	0.29	0.14
4×10^{-1}	0.18	0.08
5×10^{-1}	0.12	0.05
6×10^{-1}	0.08	0.04
8×10^{-1}	0.05	0.02
10^{0}	0.03	0.01

Table 1.18 Computed values of integral cross sections for different values of t at E = 100 GeV

t GeV^2	σ, $10^{-1}\mu$b per nucleon	
	V M D model (Sakurai)	(Kessler)
10^{-3}	95.30	85.10
1.5×10^{-3}	86.00	76.50
2×10^{-3}	80	70.50
3×10^{-3}	74.40	64.30
4×10^{-3}	68	58
6×10^{-3}	62.10	52.10
8×10^{-3}	55.80	46.20
10^{-2}	52.40	42.40
1.5×10^{-2}	44.40	35
2×10^{-2}	40	30.40
3×10^{-2}	35	24.90
4×10^{-2}	31	21.20
5×10^{-2}	28	19
6×10^{-2}	26.80	17
7×10^{-2}	24	15
8×10^{-2}	22.20	13.20
10^{-1}	20.20	11
1.5×10^{-1}	15	6.90
2×10^{-1}	12.20	4.85
3×10^{-1}	9.01	2.84
4×10^{-1}	6.93	1.93
5×10^{-1}	5.68	1.42
6×10^{-1}	4.95	1.10
7×10^{-1}	4.06	0.88
8×10^{-1}	3.55	0.71
9×10^{-1}	3.15	0.58
10^{0}	2.88	0.50

Table 1.19 Computed values of integral cross section for different values of t at E = 1 TeV

t GeV^2	σ, $10^{-1}\mu$b per nucleon	
	V m d model (Sakurai)	(Kessler)
10^{-3}	136	116
2 x 10^{-3}	119	97.70
2.5 x 10^{-3}	113	92.90
3 x 10^{-3}	109	89.10
4 x 10^{-3}	101	82
6 x 10^{-3}	93.10	73.30
8 x 10^{-3}	84.50	65.70
10^{-2}	80.40	60.60
1.5 x 10^{-2}	69.50	50.00
2 x 10^{-2}	62.50	44.70
3 x 10^{-2}	55.60	35.80
4 x 10^{-2}	50	30.20
6 x 10^{-2}	42.70	24
8 x 10^{-2}	36.20	19.20
10^{-1}	32.70	16
1.5 x 10^{-1}	24.80	10.60
2. x 10^{-1}	20.10	7.60
3 x 10^{-1}	14.80	4.56
4 x 10^{-1}	10.80	3.10
6 x 10^{-1}	8.45	1.72
8 x 10^{-1}	6.30	1.02
10^{0}	5.11	0.72
1.5 x 10^{0}	3.26	0.33
2 x 10^{0}	2.23	0.19
3 x 10^{0}	1.29	0.08
4 x 10^{0}	0.80	0.04
5 x 10^{0}	0.54	0.02
6 x 10^{0}	0.37	0.01

Table 1.20 Computed values of total cross sections for different values of primary muon energies E ϵ =0.1 GeV to 1 GeV

E GeV	σ, μb per nucleon		
	v m d model (Sakurai)	DKKN (Kobayakawa)	(Kessler)
1	1.32	2.35	1.39
1.5	2.10	3.56	2.20
2	2.72	4.38	2.82
2.5	3.28	4.90	3.40
3	3.69	5.30	3.90
4	4.23	6	4.58
5	4.71	6.50	5.05
6	5.11	7.00	5.42
7	5.50	7.40	5.80
8	5.82	7.75	6.12
9	6.12	8.08	6.38
10	6.40	8.40	6.61
20	8.41	10.10	8.41
30	9.45	11.10	9.45
40	10.10	11.70	10.10
50	10.50	12.20	10.50
60	10.80	12.70	10.80
70	11.20	12.90	11.20
80	11.40	13.20	11.40
90	11.70	13.80	11.70
100	11.90	13.60	11.90
200	13.40	15.00	13.40
300	14.30	15.70	14.30
400	15.00	16.20	15.00
500	15.50	16.80	15.50
600	15.90	17.10	15.90
700	16.20	17.40	16.20
800	16.50	17.90	16.50
900	16.90	18.10	16.85
1000	17.00	18.40	17.00

Table 1.21 Computed values of total cross sections for different values of primary energies E

ϵ_{min} = 10eV

E GeV	σ, $10^{-1}\mu b$ per nucleon				
	v m d model	D K M M	Keeler	K K	W W
2	1.90	1.90	1.40	2.90	1.46
3	3.80	4.60	3.15	6.35	3.90
4	6.60	7.38	5	9.80	6.13
5	9.50	10	6.90	13	8.20
6	12.40	12.40	8.75	16	10.20
7	15.10	14.80	10.50	19.20	12.10
8	17.80	16.80	12.30	22.20	13.90
9	20	18.70	14	25.10	15.60
10	22.30	20.50	17.81	28	17
20	38.90	35	28.40	48.50	28.50
30	49.50	44.30	37.50	63.50	37.10
40	58	51	44.20	74.50	44
50	64.50	56.50	50	84	49
60	70	62	55.50	92	53.50
70	75	67	59.50	98.50	57.50
80	79.50	71	63.50	104	61
90	83	74.50	66.50	110	64
100	86.40	78.50	70	114	67.50
200	110	102	92	152	89
300	126	120	107	174	103
400	138	132	118	195	115
500	148	143	128	210	125

Table 1.21 (contd.)

E GeV	σ, 10^{-1} μb per nucleon		
	v n d model (Sakurai)	D K M M (Kobayakawa)	(Kessler)
600	153	151	133
700	161	159	141
800	167	165	147
900	171	170	151
1000	175	174.80	156
1500	197	197	175.50
2000	210	210	189
3000	231	231	209
4000	249	249	223
5000	260	260	235
6000	270	270	245
7000	279	279	253
8000	287	287	260
9000	292	292	267
10,000	300	300	270

1.7 Discussion

The numerical calculations of theoretical results have not been previously reported in details. We have given graphical and tabular form of the computed theoretical results in the hope of making them easily accessible to experiments.

(1) Tables and graphs for the differential cross sections

Tables and graps for differential cross section $\frac{d^2\sigma}{dkdt}$, $\frac{d^2\sigma}{d\epsilon dt}$ as a function of t are given in Tables 1.1 to 1.3 & Figs. 1.5 to 1.13. These cross sections are given for a selection of E and ϵ. The selections of E is to 10 GeV, 100 GeV, and 1000 GeV and ϵ is 0.15 GeV, 0.3 GeV, 1 GeV, 3 GeV, 9 GeV, 20 GeV, 90 GeV, 100 GeV, 400 GeV, to illustrate the general trend of variations.

At E is equal to 10 GeV, the cross sections according to Kessler and v m d (Sakurai) formulations are same up to t is 10^{-3} GeV at energy transfer 0.15 GeV. From above t value of 10^{-3} GeV^2 up to the maximum value of squared four momentum transfer 10^{-2} GeV^2, the v m d prediction are slightlylow lower than Kessler prediction, maximum deviation being 15 % at the highest four momentum transfer value (Fig. 1.5)

At the energy transfer of 3 GeV (Fig. 1.6) of the same muon energy, the Kessler predictions are lower than the v m d (Sakurai) predictions, the deviations from the vmd value increasing with squared four momentum transfer

from 5 % to 70 % at t value of 10^{-2} to 1 GeV.^{2} At energy transfer of 9 GeV (Fig. 1.7) the behaviour remains the same, the difference of the Kessler values from the ν n d (Sakumai) values being falling in the range 18 % to 79 % for the variation of squared four momentum transfer from 10^{-2} GeV^2 to 1 GeV^2.

For muon energy of 100 GeV the predictions from both the formulatingsare the same for low energy transfer of 0.3 GeV (Fig. 1.8). At the energy transfer of 20 GeV (Fig.1.9) the Kessler/deviates lower than the ν n d-prediction, the difference being increasing with squared four momentum transfer to maximum of 97 % at four momentum transfer 30 GeV^2. At momentum transfer of 90 GeV (Fig. 1.10) the differenced of Kessler-prediction from the ν n d-prediction is widened, The widening of difference increases with increasing squared four momentum transfer value. The maximum difference at maximum squared four momentum transfer (100 GeV^2) is 99.6 %.

/ prediction

For muon energy of 1 TeV (Fig. 1.11 & 1.12) predictions from both formulations are same for all squared four momentum transfer values up to 3 x 10^{-3} GeV.^{2} At energy transfer of 100 GeV (Fig. 1.12), the Kessler-predictions deviate lower and gradually increases with the squared four momentum transfer. At 400 GeV (Fig.1.13) energy transfer from muon energy of 1 TeV the ν n d (Sakurai) cross section is higher by 99.7 % when t is 100 GeV^2.

(ii) Tables and graphs of differential cross sections

For an illustrative set of muon energies 10 GeV, 100 GeV, and 1000 GeV the predicted differential cross sections $\frac{d\sigma}{d\epsilon}$ according to DKMN (Kobayakawa - 1967), Kessler (1965), v m d (Sakurai - 1969) formulations are given in tables 1.4 to 1.9 and displayed in figures 1.14 to 1.19.

For 10 GeV (Fig. 1.14) muon energy, the Kessler cross sections closely agree with v m d (Sakurai) cross sections in the energy transfer range 0.15 GeV to 1 GeV. The DKMN(Kobayakawa) values at energy transfer of 0.15 GeV greater than the v m d (Sakurai) value by 30 % which gradually decreases to zero and then at 1 GeV, DKMN (Kobayakawa) value is smaller than the v m d (Sakurai)value. Above 1 GeV (Fig. 1.17) of energy transfer the DKMN (Kobayakawa) values lie in between v m d (Sakurai) values and smaller Kessler values. The differences among v m d, Kessler and DKMN values are 58 % and 48 % respectively, at energy of 9 GeV.

The behaviour of cross section among the three formulations is more or less the same below the energy transfer of 1 GeV and the above 1 GeV for higher muon energies illustrated (Figs. 1.15, 1.16, 1.18 & 1.19).

The difference of v m d cross sections from Kessler values gradually increases with increasing energy transfer. With increasing muon energy DKMN(Kobayakawa) values come closer to v m d (Sakurai) values.

At muon energy of 1 TeV (Fig. 1.19) the values predicted by DKMN (Kobayakawa) and v m d (Sakurai) formulations are same for energy transfers from 1 GeV to 10 GeV and then there is little deviation which increases to 25 % at energy transfer of 900 GeV.

(iii) Tables and graphs for $\frac{d\sigma}{dt}$

The values of cross sections differential in squared four momentum transfer have also computed. A set of data for selected three muon energies are given in the table 1.10 to 1.12 and displayed graphically in Figs. 1.20 to 1.22 . The predicted values according to Kessler and v m d (Sakurai) formulations are the same for values of squared four momentum transfer below about 0.02 GeV^2. For higher squared four momentum transfers, Kessler values are smaller than the v m d (Sakurai) values. The deviation between the two predictions increases with the increase of squared four momentum transfer for the fixed values of muon energies and also increases with increasing muon energies at fixed values of squared four momentum transfers.

(iv) Table and graphs of integral cross sections σ

Integral cross sections are obtained numerically by integrating $\frac{d\sigma}{d\epsilon}$ and $\frac{d\sigma}{dt}$ cross sections separately for the various muon energies up to 10TeV. These are presented in tables 1.13 to 1.19 and shown graphically in Figs. 1.23 to 1.29. The general

trend of behaviour of integral cross sections among the formulations is the same as those observed for differential cross sections. For higher muon energies (Figs. 1.15 & 1.16), the DKMN and v m d (Sakurai) predictions gradually approach to close agreement for higher values of energy transfer.

Integral cross section $\sigma(E,t)$ according to Kessler formulation deviates from v m d prediction gradually to lower and lower values, with the increasing t' difference at 1 GeV^2 of lower value of the squared four momentum transfer being 80 % in case of 100 GeV/ The trend /muon of behaviour is same for lower and higher muon energies.

(v) Tables and graphs for total cross-sections $\sigma(E,>\epsilon)$ vs muon energy E.

The nature of variation with muon energy of the total cross-sections according to various formulations is presented graphically in Fig. 1.30 - 1.32. The numerical data for these cross-sections are given in the tables 1.20 - 1.21. Here also it is seen that for energy transfer range 0.15 GeV to 1 GeV DKMN predictions are much higher than v m d & Kessler predictions which are in close agreement. For energy transfer range 1 GeV, the Kessler-values are lower than DKMN and v m d / which / values gradually approach to agreement above the muon energy of 500 GeV.

(vi) The ratio of integral cross sections

In figures 1.33 tp,1.37 we have plotted ratios of integral cross sections according to various formulationsf the ratio being taken relative to v m d (Sakurai) cross sections.

These graphs demonstrate clearly the relations among the various cross sections for both energy transfers and muon energies.

Differential cross sections $\frac{d^2\sigma}{d\epsilon dt}$ and $\frac{d\sigma}{dt}$ and the integral cross sections $\sigma(E,t)$ values according to DKMN formulations have not been included in the data presented above. As expected, the predictions of DKMN and other two agree at very low values of squared four momentum transfer. The deviation among the predictions begins above the squared four momentum of the order of 10^{-3} GeV^2, for the whole range of muon energies and the DKMN cross sections lie between v m d (Sakurai) and Kessler-values.

The v m d model approximation differential cross section formula (1.61) with 't_0' = m_ρ^2 = 0.564 GeV^2 appears closer in form to that of Kessler under the hypothesis of factorization (1.46) and with t_0= 0.365 GeV^2. In the present work we have chosen the Kessler's form-factor formula. Kobayakawas proposal (1.52) mixed 10 % of the point nucleon contribution with the nucleon structure contribution under the DKMN approximation with t_0 =0365 GeV^2. At energy transfer greater than the squared four momentum transfer, the DKMN transverse virtual photon flux is very close to that of Kessler and both formulations have been considered with the same proposal for the form factor. The v m d proposal (1.79) has a different dependence on the squared four momentum transfer and implies a different

character of virtual photon interaction with nuclear matter. We have not considered for evaluation the more detailed expression (1.78) of the v m d model, because the statistical precision of the available experimental data is inadequate to choose between the two forms.

meson/ The vector/dominance calculation was done also by Tsai (1969). This and other models(constant q^2- sum rule, Parton model and Regge exchange trajectory) for calculations of lepton-nucleon interaction process are not included in this work. In Parton model, the lepton scatters incoherently from the point like constituents inside the proton and the result for W_2 is a universal function depending only on the ratio of energy transfer to the squared four momentum transfer. Regge exchange trajectory model (1969) approach leads to a form for W_2 different from that of the Parton model. These models are not yet sufficiently tractable for numerical computation application in experiments.